

THE MECHANISM OF CORROSION INHIBITION
BY ORGANIC AMINES AS INTERPRETED
BY OHMIC RESISTANCE FILM

By

ALLAN PHILLIP DAVID
II

Bachelor of Applied Science
University of Toronto
Toronto, Ontario, Canada
1950

Master of Applied Science
University of Toronto
Toronto, Ontario, Canada
1951

Submitted to the faculty of the Graduate School
of the Oklahoma State University of Agriculture
and Applied Science in partial fulfillment
of the requirements of the degree of
DOCTOR OF PHILOSOPHY
May, 1959

NOV 18 1959

THE MECHANISM OF CORROSION INHIBITION
BY ORGANIC AMINES AS INTERPRETED
BY OHMIC RESISTANCE FILM

Thesis Approved:

Scott P. Ewing

Thesis Advisor

G. N. Madley

John B. West

A. Shuman

Tom E. Moore

Robert Macdonald

Dean of the Graduate School

430733

PREFACE

Although organic corrosion inhibitors are in widespread use and their effectiveness is conceded, especially in the protection of iron or ferrous alloys in acidic solutions, the mechanism of inhibition is obscure and disputed. For this reason, the screening of inhibitors has been trial and error.

To assist in the comprehension of inhibition and to provide a sound basis for selection of inhibitors, I have attempted to relate the mechanism of inhibition to an adsorbed film of inhibitor on the surface of the metal offering an ohmic resistance to the corrosion current.

I wish to express my sincere appreciation to Dr. S. P. Ewing, my major advisor, whose assistance and understanding was primal in the success of this research; to the other members of my committee for their guidance; to Dr. Franklin Graybill for his aid in statistical analyses; to the Research Apparatus Development Laboratory for their excellent service in equipment building and maintenance; and to the Jersey Production Research Center of Tulsa whose financial support facilitated the successful completion of this work.

TABLE OF CONTENTS

Chapter	Page
I. INTRODUCTION	1
Limitation of the Study	5
Review of the Literature	5
II. METHOD AND PROCEDURE	12
Apparatus	12
Experimental Procedure	16
Static Corrosion Testing	23
III. RESULTS	26
Polarization Data	26
Static Corrosion Tests	36
IV. INTERPRETATION OF RESULTS	38
V. SUMMARY AND CONCLUSIONS	50
Suggestions for Future Work	52
BIBLIOGRAPHY	53
APPENDIX A	56
APPENDIX B	62

LIST OF TABLES

Table	Page
I. Calculated Resistances on 5.0 cm ² Electrode From Polarization Data	31
II. Effect of Concentration on r_a/r_c	39
III. Calculated Corrosion Currents and Inhibitor Effectiveness Based on Resistance Film and pH	42
IV. Observed and Calculated Potentials Based on Adsorption and Basicity of Inhibitors	44
V. Relative Order of Basicity and Size of the Amines Arranged in Descending Order of Inhibitor Effectiveness	47
VI. Experimental Current-Potential Relationships	63
VII. Experimental Current-Potential Relationships	65
VIII. Experimental Current-Potential Relationships	66
IX. Experimental Current-Potential Relationships	70
X. Experimental Current-Potential Relationships	72
XI. Experimental Current-Potential Relationships	74
XII. Experimental Current-Potential Relationships	76
XIII. Composite Tabulation of Data for Calculating Resistances Per Unit Area	78
XIV. Composite Tabulation of Data for Calculating Resistances Per Unit Area	79
XV. Composite Tabulation of Data for Calculating Resistances Per Unit Area	81
XVI. Composite Tabulation of Data for Calculating Resistances Per Unit Area	82

LIST OF TABLES (Continued)

XVII.	Composite Tabulation of Data for Calculating Resistances Per Unit Area	83
XVIII.	Composite Tabulation of Data for Calculating Resistances Per Unit Area	84
XIX.	Composite Tabulation of Data for Calculating Resistances Per Unit Area	85
XX.	Analysis of Variance of Resistance Per Unit Area . .	86
XXI.	Analysis of Variance of Resistance Per Unit Area . .	87
XXII.	Analysis of Variance of Resistance Per Unit Area . .	88
XXIII.	Analysis of Variance of Resistance Per Unit Area . .	89
XXIV.	Analysis of Variance of Resistance Per Unit Area . .	90
XXV.	Analysis of Variance of Resistance Per Unit Area . .	91
XXVI.	Analysis of Variance of Resistance Per Unit Area . .	92
XXVII.	Weight Losses of Armco Iron Strips in Static Tests .	93

LIST OF ILLUSTRATIONS

Figure	Page
1. Experiment Cell	13
2. Hickling Current Stabilizer	15
3. Electrical Circuit for Polarization runs	21
4. Cathodic Polarization of Iron Electrode	27
5. Anodic Polarization of Iron Electrode	27
6. Cathodic Polarization of Iron Electrode	28
7. Anodic Polarization of Iron Electrode	28
8. Cathodic Polarization of Iron Electrode	29
9. Anodic Polarization of Iron Electrode	29
10. Cathodic Polarization of Iron Electrode	30
11. Anodic Polarization of Iron Electrode	30
12. Cathodic Current--Potential Relationship for Determina- tion of $E_o - E_i/i_e$	32
13. Anodic Current--Potential Relationship for Determina- tion of $E_o - E_i/i_e$	32
14. Relationship Between Resistance Per Unit Area and Amine Concentration	33
15. Relationship Between Resistance Per Unit Area and Amine Concentration	33
16. Relationship Between Resistance Per Unit Area and Amine Concentration	34
17. Relationship Between Resistance Per Unit Area and Amine Concentration	34
18. Relationship Between Resistance Per Unit Area and Amine Concentration	35

LIST OF ILLUSTRATIONS (Continued)

19.	Relationship Between Resistance Per Unit Area and Amine Concentration	35
20.	Relationship Between Resistance Per Unit Area and Amine Concentration	36
21.	Weight Loss of Samples in Inhibited Solutions (0.01% N) with Time	37
22.	Weight Loss of Samples in Inhibited Solutions (0.05% N) with Time	37
23.	Variation of Adsorption Potential Shift with Concentration	46
Plate		
I.	Static Corrosion Cells	17
II.	Experimental Polarization Set-Up	20

CHAPTER I

INTRODUCTION

In the field of corrosion inhibition certain chemicals when added to normally corrosive liquid media will inhibit the corrosion of metals in these media. Additions of soluble hydroxides, chromates, phosphates, silicates and carbonates decrease the corrosion rate of iron and other metals in aqueous solutions by anodic inhibition, keeping in repair or forming a protective film on the metal surface. Magnesium, zinc or nickel salts react at cathodic areas to form insoluble hydroxides over the surface as a barrier to further reduction of oxygen in the cathodic reaction.

In this field, polar organic substances and colloids have found use as inhibitors of corrosion, especially in acid solutions. These include the nitrogen containing compounds such as aliphatic and aromatic amines, pyridine, quinoline and acridine and their substitution products; oxygen containing compounds such as aldehydes, ketones and organic acids; sulfur containing compounds, usually the mercaptans. Of these, the amines are in most general use and are incorporated in many of the commercial inhibitors.

Inhibition by organic chemicals has been explained on the basis of retardation of the cathodic or anodic process similar to inorganic inhibitors. Because of the positive charge associated with an amine, an electrostatic attraction between the cathodic

areas on the metal and the amine has been postulated as a mechanism for adsorption of the inhibitor on the metallic surface. On the other hand, inactivation of electrons of the metallic surface and prevention of electron flow by a complexing reaction would inactivate anodic areas. In the first instance as a so-called cathodic inhibitor, the cathodic reaction, hydrogen evolution, would be retarded, i.e., an increase in hydrogen overvoltage. In the second case as an anodic inhibitor, the anodic reaction, metal dissolution, would be retarded, in effect a passivation phenomenon. A third mechanism, involving general adsorption of the inhibitor blanketing the surface and offering an ohmic resistance to local action current introduces the concept of mixed inhibition.

The mechanism of inhibition has been explained in different ways by different investigators. An enigma still exists as to the mechanism; therefore, the purpose of this work is the investigation of one of the theories, namely, that of ohmic resistance, to determine if there is correlation between resistance and inhibition.

The resistance of an adsorbed film cannot be measured directly with any degree of accuracy, but may be calculated indirectly using measurable quantities.¹ In a freely corroding electrode, the local action current follows the simple Ohm's Law relation

$$i_L = \frac{E_c - E_a}{R_a + R_c} = \frac{\frac{E_c - E_a}{r_a} + \frac{E_c - E_a}{r_c}}{\frac{A_a}{A_c}} \quad (1)$$

¹See Appendix A for complete derivation.

where subscripts denote cathodic and anodic sites. For maximum current flow, the rate of change of i_L with respect to the anodic area A_a is zero, (assuming that the total area is made up of anodic and cathodic areas only with no insulated spots, i.e., $A_a + A_c = 1$), $\frac{di_L}{dA_a} = 0$

$$\text{then } \frac{r_a}{r_c} = \frac{(A_a)^2}{(A_c)^2} = \frac{(E_o - E_a)^2}{(E_c - E_a)^2} \quad (2)$$

When a current i_e is applied to a corroding coupon, the resulting potential is:

$$E_i = E_o - i_e \frac{R_a R_c}{(R_a + R_c)} \quad (3)$$

where

$$\frac{R_a R_c}{R_a + R_c} = \sqrt{r_a r_c} \quad (4)$$

and therefore,

$$\sqrt{r_a r_c} = \frac{E_o - E_i}{i_e} \quad (5)$$

The solution of (2) and (5) yields the relationships:

$$r_a = \frac{E_a - E_o}{E_o - E_c} \times \frac{E_o - E_i}{i_e} ; \quad r_c = \frac{E_o - E_c}{E_a - E_o} \times \frac{E_o - E_i}{i_e} \quad (6)$$

from which a resistance type measurement may be determined for cathodic and anodic areas.

The terms R_a and R_c are resistances in series to local action current. A direct measurement of resistance of a film by impressed current does not give a true picture since anodic and cathodic resistances are in parallel to impressed current. By the

very nature of resistances in parallel, an increase in R_a and/or R_c would show only a small increase in resistance with respect to impressed current, whereas a large increase may actually exist with respect to the corrosion current. This means that separation of the resistance terms is necessary. This, in effect, is what has been accomplished by equation (6).

Assuming that the anodic reaction is dissolution of iron to ferrous ion, and the cathodic reaction the evolution of hydrogen, then:

$$E_a = -0.685 + 0.0295 \log (F_{e^{++}}) \quad \text{and} \quad (7)$$

$$E_c = -0.244 - 0.0591 \text{ pH} \quad (8)$$

By fixing the concentration of ferrous ion and measuring pH, the terms E_a and E_c are determined by the above Nernst relationships (expressed in terms of the saturated calomel electrode).

The quantity $\frac{E_o - E_i}{i_e}$ is the slope of the line relating

impressed current to the resulting potential E_i where $E_i = E_o$ at $i_e = 0$. A linear relationship is obtained at low current densities in the region where the polarized potential is close to the corrosion potential (23).

Previous investigations on organic inhibitors have been done using highly corrosive media such as sulfuric acid. That organic compounds are applicable in mildly corrosive media is evidenced by the great quantity of these available on the market for corrosion inhibition in other than pickling operations. With this in mind, and also the fact that in practice, corrosion for

the most part occurs in other than highly acidic solution, a relatively mild corrosive environment was selected for the study. Since corrosion by dissolved carbon dioxide is of practical importance, especially in the petroleum industry, the investigation in this dissertation was carried out in a water solution saturated with carbon dioxide at 25° C.

Limitations of the Study

To evaluate the applicability of the ohmic resistance theory, the current-potential relationship was determined only at low current densities. A comprehensive coverage of the problem would entail considerably higher current densities to determine the Tafel constants for investigation of the hydrogen overvoltage theory.

Review of the Literature

The investigation of organic inhibitor mechanism has been so extensive that it would be impracticable to cite comprehensively all published material. Rather, the more recent and the most pertinent literature will be offered emphasizing the conflicting arguments.

The adsorption of an inhibitor, either chemically or physically, by the metal is generally accepted. Mann, Lauer and Hultin (17) stated that in a solution containing ammonium or ammonium-like ions, the positive iron ions released by a corroding iron sample are replaced on the metal by the ammonium ions analogous to the hydrogen ion replacement in corrosion. Unlike the

hydrogen ion type of replacement in which depolarization is effected by the neutralization and release of hydrogen gas, the ammonium ions are held to the negative surface of the metal and form a double ionic layer, acting as a protective layer. That this was an adsorption phenomenon was shown by the straight lines obtained in the logarithmic plot of percent effectiveness in reducing corrosion versus inhibitor concentration in percent nitrogen. The covering power of an amine inhibitor and hence its effectiveness at low concentrations was explained in terms of the stereochemistry of the molecule.

In early work on organic inhibitor mechanism, Chappel et al (4) adduced the effect on hydrogen overvoltage by a blanketing of discharged inhibitor adsorbed on cathodic areas. They measured hydrogen evolution in inhibited and non-inhibited solutions noting a diminution of hydrogen evolution in the inhibited solution. They further substantiated their theory by current-potential measurements noting that cathodic potentials were affected to a greater degree by inhibitor than were anodic.

Rhodes and Kuhn (22) using heterocyclic organic compounds of nitrogen based the inhibiting power of these compounds on the percentage decrease in rate of formation of hydrogen by the action of dilute sulfuric acid on iron. They found that cyclic compounds containing an atom of nitrogen in the ring were the most efficient. Increasing molecular weight by the addition of alkyl, phenyl or amine groups increased the inhibiting action with the most efficient inhibitors being derivatives of acridine. They attempted to measure an interfacial resistance layer formed by the adsorbed

inhibitor on the metal by using an impedance bridge and an A.C. source with the cell in one leg of the bridge. They found there was a small increase in resistance with the addition of inhibitor but could not quantitatively relate inhibiting efficiency and resistance. They concluded that inhibiting action was not due solely to the resistance of the film but to some specific property of the adsorbed film. That the authors realized only a small increase in resistance may be attributed to the fact that with the type of apparatus used a composite parallel resistance was measured. In actuality, the resistance of interest is made up of two series resistances.

The resistance film theory of inhibition and general adsorption over the whole metal surface was asserted by Machu (16) in the pickling of iron in sulfuric acid. He protested the preferential adsorption on cathodic sites by reference to the dissolution of oxide scale, which is cathodic to base metal, and the protection of bare metal in inhibited solution, and averred that a resistance film of three ohms was sufficient for protection. Machu gave no details as to the experimental procedure other than that current-potential relationships were determined. He obtained a linear relationship between applied voltage and current and noted an increase in slope with the addition of inhibitor. However, with the range of currents used (0.1 to 0.5 amp/cm²), Machu was beyond the range of linearity. He admitted to oxygen evolution in his anodic curves and, therefore, his data lie in the Tafel region, which region is semilogarithmic in the relation between logarithm of the current and potential (25). What Machu called resistance

should have been determined as the Tafel slope.

Bockris and Conway (2), on the other hand, found that hydrogen overvoltage on iron increased on addition of organic corrosion inhibitors and decreased on the addition of activators. Measurements were made with an electronic commutator in which the working electrode is connected alternately with the polarizing circuit and the measuring circuit. Therefore, when the potential of the electrode is actually being measured no polarizing current is flowing. The authors found there was negligible ohmic overvoltage and, therefore, discounted the adsorbed film theory. The indirect or commutator method introduces error in the determination of potential in that the electrode potential will decay on cessation of polarizing current and the true polarized potential will not be obtained.

Elze and Fischer (5) confirmed the raising of activation overvoltage for hydrogen evolution in their polarization studies of iron in hydrochloric acid. They found that metal solution overvoltage was little affected by inhibitors.

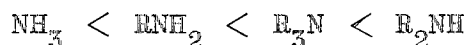
Hoar (15) measured the effect of various inhibitors on the corrosion potential of mild steel in ten percent sulfuric acid solution. He found that in most cases the corrosion potential was increased in the noble direction. On the basis of this alone, he concluded that organic inhibitors affected the anodic reaction to a greater extent than the cathodic. His technique for measuring potentials was unique in that the liquid junction between the corroding sample and the $\text{Sb}/\text{Sb}_2\text{O}_3$ half cell consisted of a strip of filter paper moistened with electrolyte and strung between the

corrosion cell and the antimony half cell. The anomaly in Hear's findings was the fall in potential to a less noble value for additions of o-tolylthiourea which, based on his criterion for adsorption, indicates that initially this inhibitor is cathodic. No correlation between potential shift and inhibitor effectiveness could be established. The inhibitor which was 98 percent effective shifted the potential only + 8 millivolts. Another, which was 93 percent effective, shifted the potential + 63 millivolts.

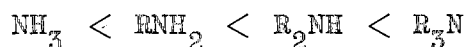
By far the most comprehensive treatment of the subject of inhibitors has been given by Hackerman and his associates (7), (8), (9), (10), (11), (12), (13), (14). Early work (12), (13), dealt with the mechanism of adsorption of the inhibitor on the metal surface. It was found that curves of electrode potential plotted against inhibitor concentration could be fitted to an equation based on the Langmuir isotherm. Adsorption and desorption studies (8) of organic acids, amines, and esters in benzene solution on SAE 1020 steel powder showed that some portion of the sorbed material could not be desorbed by fresh solvent. Acids and amines were adsorbed to a greater extent than esters. Further adsorption studies along the same lines for dodecyl compounds (10) included data on inhibiting power. It was found that diamines were adsorbed through both amine groups; amine salts were not as effectively adsorbed as amines; high molecular weight quaternary salts were strongly adsorbed. Inhibitor effectiveness was based on rate of hydrogen evolution from the inhibited solutions as compared with the rate from the uninhibited solution. These measurements showed that quaternary salts were the most effective inhibitors followed

by diamines, monoamines and monoamine acetates.

On the basis of his previous work and the findings of others, Hackerman discussed the action of organic inhibitors (11). In his paper, inhibition is explained as resulting from increased resistance to current flow caused by electrostatic adsorption at cathodic areas and from anodic polarization caused by chemisorption--the relative contribution of each depending upon the inhibitor. Chemisorption at anodic areas is looked upon as complex formation in situ since many compounds (including ammonia type) are capable of forming complexes with metal ions. In this instance, complexing is effected not with the free ion in solution but with the metal ion on the surface as postulated by the free electron theory of solids. The strength of the iron-amine bond is a function of the electron density on the nitrogen atom and the availability of those electrons for coordinate bond formation. The basicity of the amine was taken as the basis for the electron density. The relative order of inhibitor effectiveness of aliphatic amines was given as



where R is methyl and



where R is ethyl, propyl, butyl, or amyl.

A Pearson Null Bridge was tested as a quantitative tool for evaluating inhibitors (9) since changes in polarization characteristics of a metal may be determined by this method. Hackerman found that results with this bridge gave about 70 percent correla-

tion with other methods as far as inhibiting mechanism was concerned. He concluded that the bridge in its present form was not applicable as an instrument for inhibitor evaluation.

Hackerman discussed the physico-chemical aspects of corrosion inhibition in general, in a purely qualitative way, expressing the views and findings of researchers in this field in terms of kinetics, solution chemistry, interfacial phenomena, etc., (7). He concluded that the divergent views were not irreconcilable but that, because of the complexity of corrosion on the whole, and the specificity of certain corrosion problems, a universal inhibitor may not be possible, but rather each circumstance may require its own "prescription".

CHAPTER II

METHOD AND PROCEDURE

Apparatus

Electrolytic Cell

The H shaped experimental cell was fabricated of glass, the legs of the H forming the separate anode and cathode compartments. (See Figure 1) A disc of fritted glass was sealed midway in the cross bar of the cell to maintain a liquid junction between the compartments, and to prevent reaction products from the auxiliary electrode reaching the compartment containing the experimental electrode.

The auxiliary electrode was a platinum mesh cylinder and was positioned in one cell compartment by a rubber stopper.

The experimental electrode was a one inch diameter by one inch cylinder of Armco iron sealed in Armstrong's C₇ epoxy plastic to expose only one circular face. Electrical connection was made by soldering a one-eighth inch copper tube to the iron electrode. The copper tube was bent in such a way as to position the iron specimen with the exposed face up. The copper tube was encased in plastic to form an inert stem for fixing the electrode in the cell.

To insure saturation of the electrolyte with CO₂ and

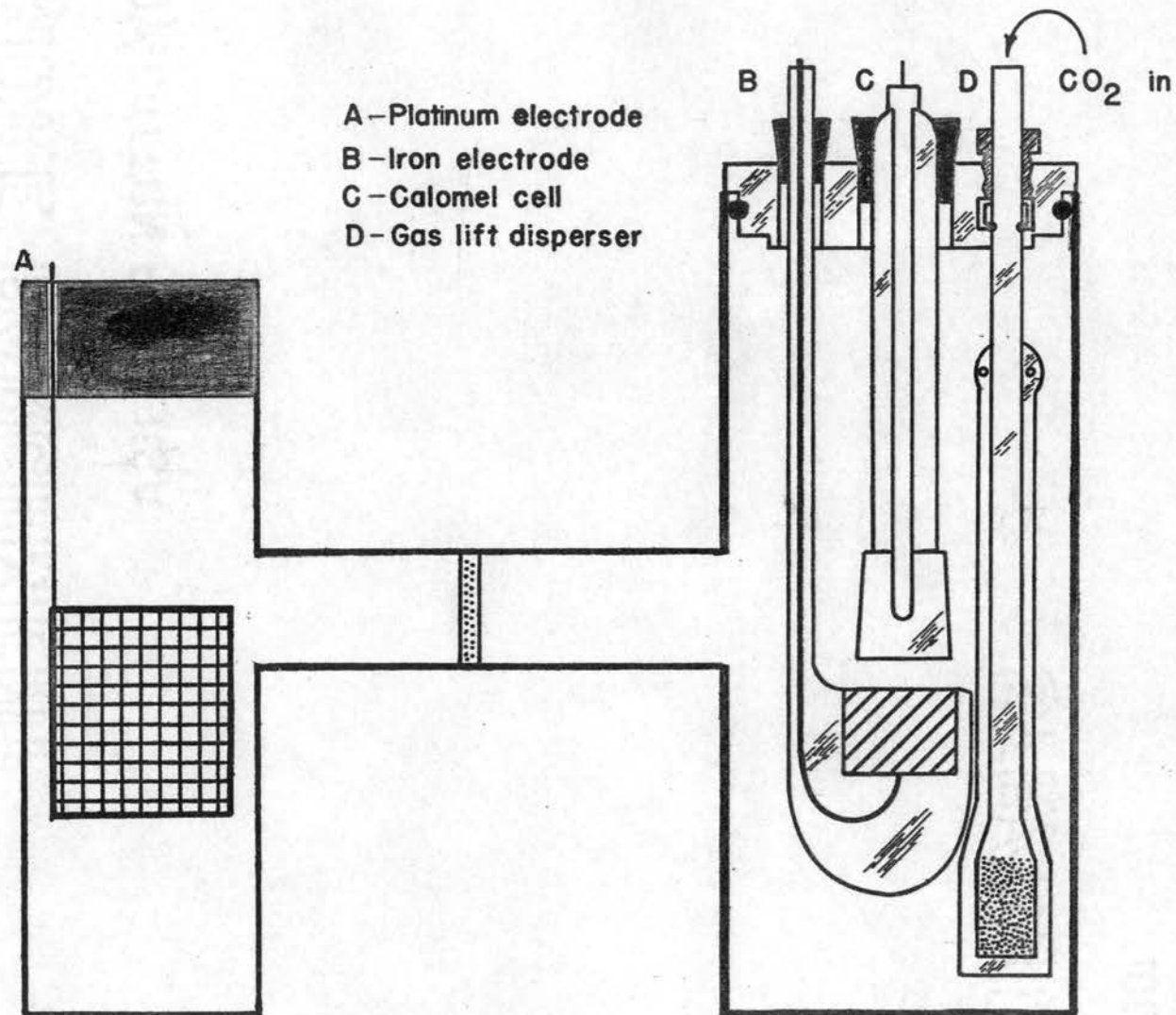


FIGURE 1 - Experimental cell

prevent impingement of CO₂ bubbles on the electrode surface, as well as to provide agitation of the electrolyte, the air lift principle was utilized. This was effected by sealing a section of glass tubing around a fritted glass stick disperser through which CO₂ was passed.

The iron electrode, gas disperser and Beckman 8970 calomel electrode were positioned in the larger compartment of the cell through an O-ring gasketed plexiglass cover. The two electrodes were fitted through the cover by rubber stoppers, the glass disperser by a small O-ring and threaded nut which acted as a mechanical seal against the O-ring.

Current Stabilizer

The stabilizer circuit developed by Bruce and Hickling (3) was modified by changes in components to cover a current range of 10 to 250 microamperes. (See Figure 2).

Auxiliaries

1. A Leeds and Northrup No. 7655 Potentiometer was used to measure the potential difference between the saturated calomel electrode and the iron electrode for various impressed currents.

2. A 200 v. D.C. power supply acted as the current source for the cell.

3. A Simpson Volt-Ohm-Microammeter Model 269 was used to measure the impressed currents in the electrolytic cell.

Corrosion Cell - (Static Test)

One quart Mason jars fitted with No. 14 rubber stoppers were used in determining the corrosion rate of Armco iron samples in inhibited carbonic acid solutions. Four strips, one inch by

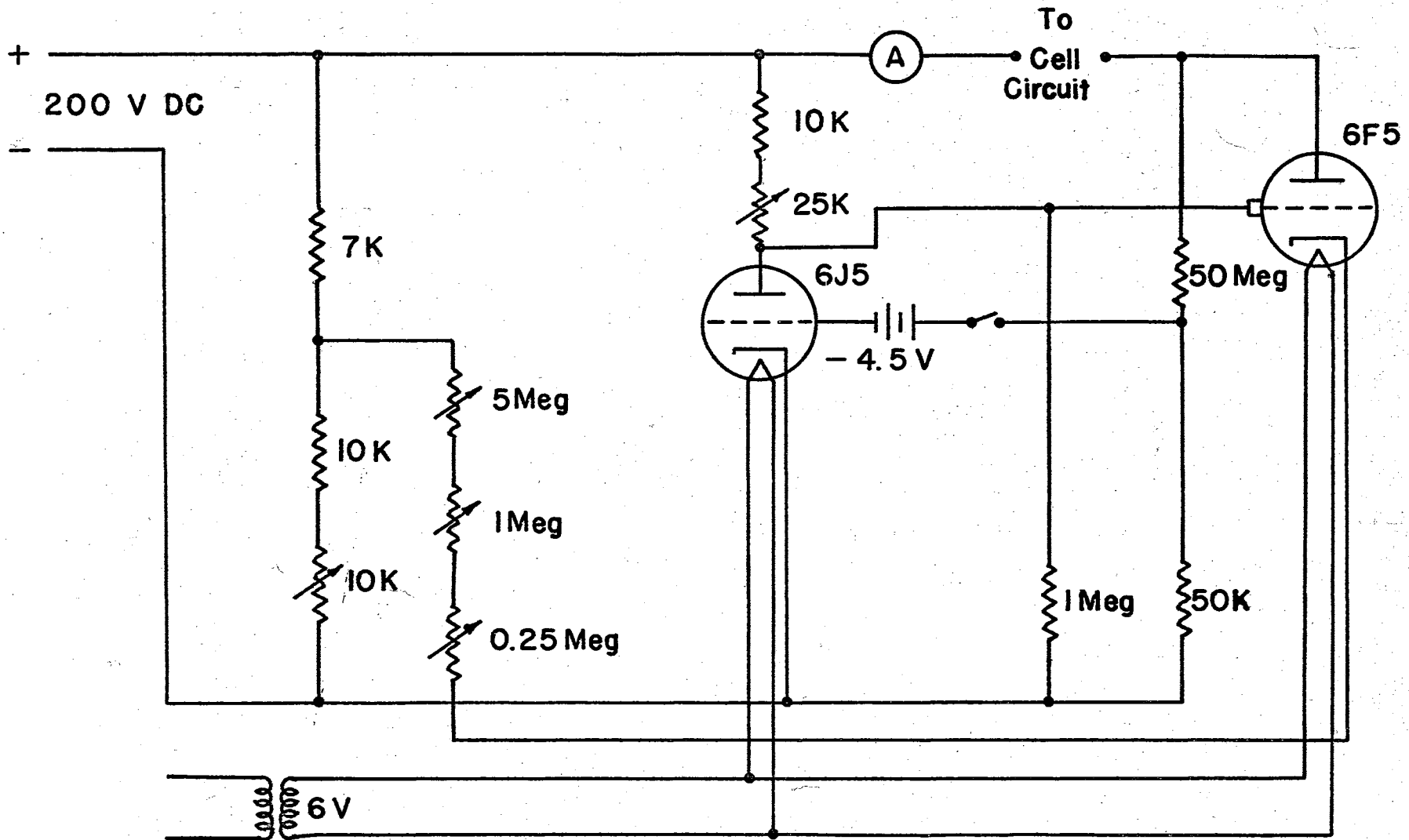


FIGURE 2- Hickling current stabilizer

three inches by twenty-five mils thickness were suspended from the stopper by glass hooks. (See Plate I) A fritted glass stick disperser and close fitting glass tube chimney surrounding the stick disperser were incorporated to keep the solution saturated with respect to CO_2 .

Experimental Procedure

Electrolyte Preparation

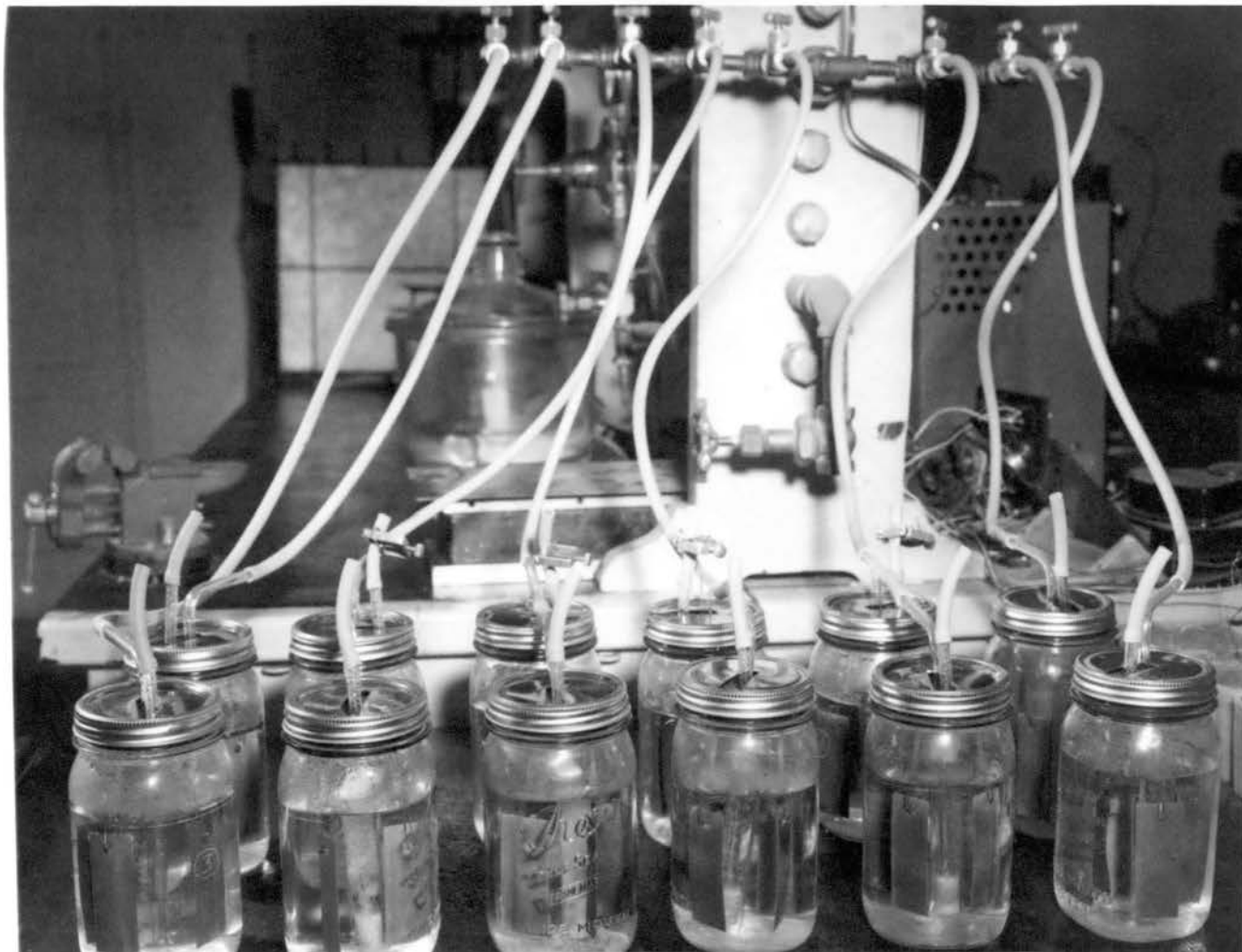
The carbonic acid solution was prepared by redistilling distilled water to which potassium permanganate was added to oxidize the impurities. To insure the absence of oxygen, the distillation was carried out under a nitrogen blanket in the distillation flask; CO_2 which was passed over hot copper turnings to remove oxygen was bubbled through the distillate as it was collected in one gallon polyethylene bottles packed in ice. In this manner, air free carbonic acid solution was made directly, warranting a solution saturated with CO_2 at 25°C . The solution was kept refrigerated until ready for use.

To determine the oxygen content of the electrolyte, a Winkler test (27) was run on the solutions. These tests showed an average oxygen content of about 0.2 p.p.m. This can be compared with water at 25°C . saturated with air which contains 7.2 p.p.m. oxygen.

Electrode Preparation

The experimental electrode described previously was used throughout the research. The electrode was recast in plastic when

PLATE I
Static corrosion cells



the plastic showed a tendency to pull away from the iron specimen.

Preparatory to a run, the iron surface was abraded by a file and 240 C emery paper, and polished with 4/0 emery paper. The surface was then cleaned with acetone and etched for one minute in a 1:3 by volume HNO_3 -water etching solution. Following the etch, which gave a well defined crystalline surface, the electrode was scoured, rinsed and stored in a vacuum dessicator for one hour.

Cell Preparation

All components of the cell were thoroughly cleaned prior to a run. Any contaminant, especially amine from a previous run, adversely affected the succeeding run. All glass components were cleaned with HCl and chromic acid, thoroughly rinsed with distilled water and dried.

To fill the cell with electrolyte, the cell was fitted with the components as illustrated in Figure 1. The cell was evacuated and purged with CO_2 a number of times ending with an atmosphere of CO_2 in the cell. Saturated carbonic acid solution was transferred from the storage polyethylene bottle by a tygon tube connection through the plexiglass top. To expedite the transfer, suction was applied to the cell and CO_2 bubbled into the polyethylene bottle. When 650 ml. had been transferred to the larger compartment (as determined by an etched line on the cell), the CO_2 was started through the air lift disperser. Ferrous chloride was added finally to give 0.01 molar in ferrous ion. The cell was then put in a thermostatically controlled water bath ($25^\circ\text{C} \pm 1^\circ\text{C}$) and allowed to remain twelve hours to attain equilibrium.

Except for dimethylaminoethanol and morpholine which were redistilled to give a colorless, constant boiling product, all the amine inhibitors were reagent grade as supplied by the manufacturer.

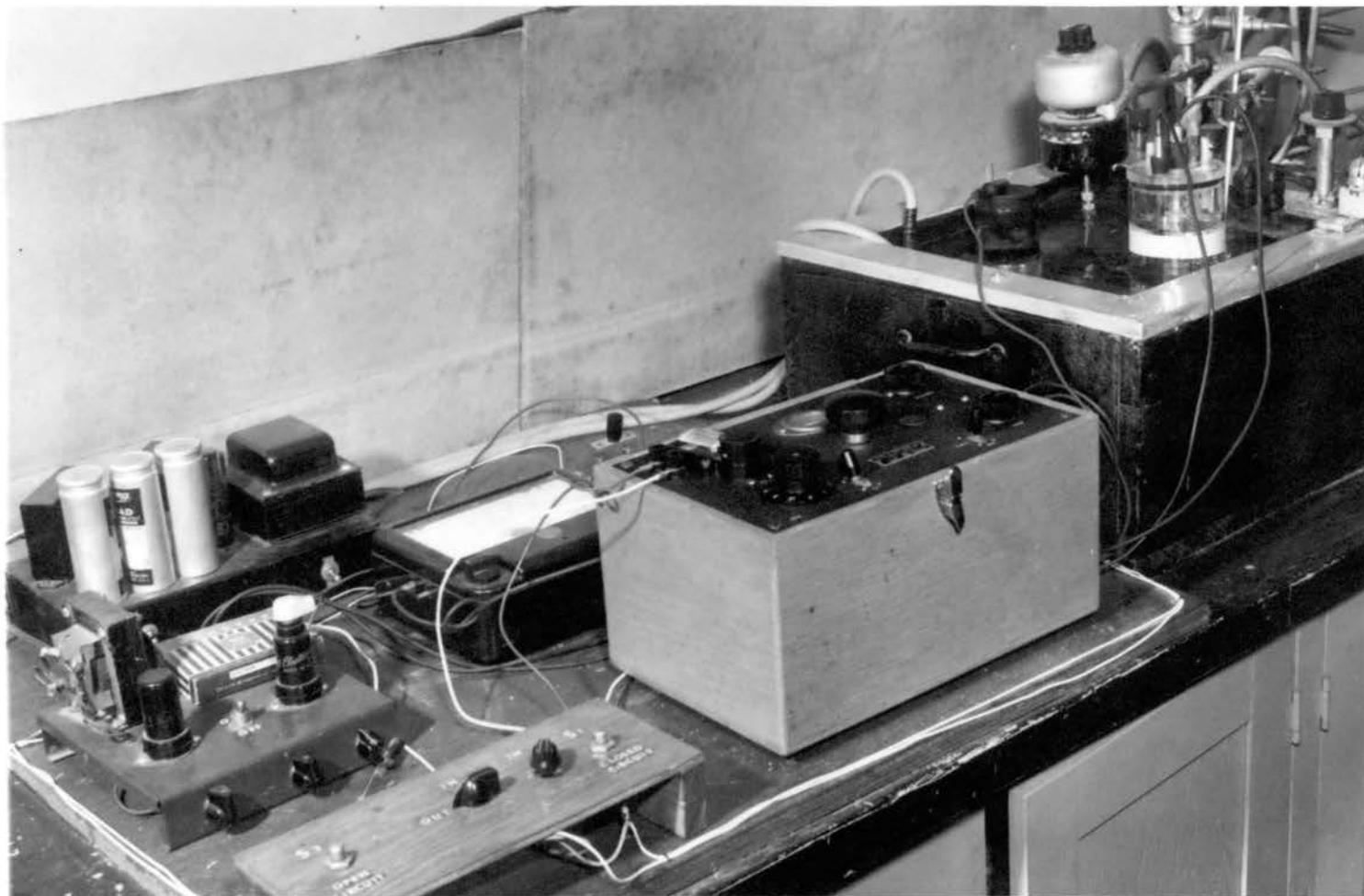
Polarization Runs

The cell was placed in the thermostatically controlled temperature bath as shown in Plate II and connected into the electrical and measuring circuit as illustrated in Figure 3. The iron electrode could be made the anode or cathode by the double pole double throw knife switch. The constant current device was capable of delivering from 10 to 200 μ amperes; therefore, to extend the range to zero the variable 1.1 megohm resistor was installed to shunt all or part of the current as required.

A run consisted of impressing a series of currents between the platinum electrode and the iron electrode and measuring the resulting potential between the iron electrode and the calomel cell.

The current-potential relationship for the iron was determined for the electrode in carbonic acid (control run), and in carbonic acid containing inhibitor in concentrations of 0.01, 0.02 and 0.05 weight percent based on nitrogen present in the amine used as the inhibitor (19). For example, in the control run the iron was made cathodic at currents of 0, 2, 5, 8, 12, 17 and 20 μ amperes, then run anodic at the same currents. Then inhibitor was added to give the required concentration and the procedure was repeated. In this manner, current-potential relationships could be compared between no inhibitor and the various additions of inhibitor,

PLATE II
Experimental polarization set-up



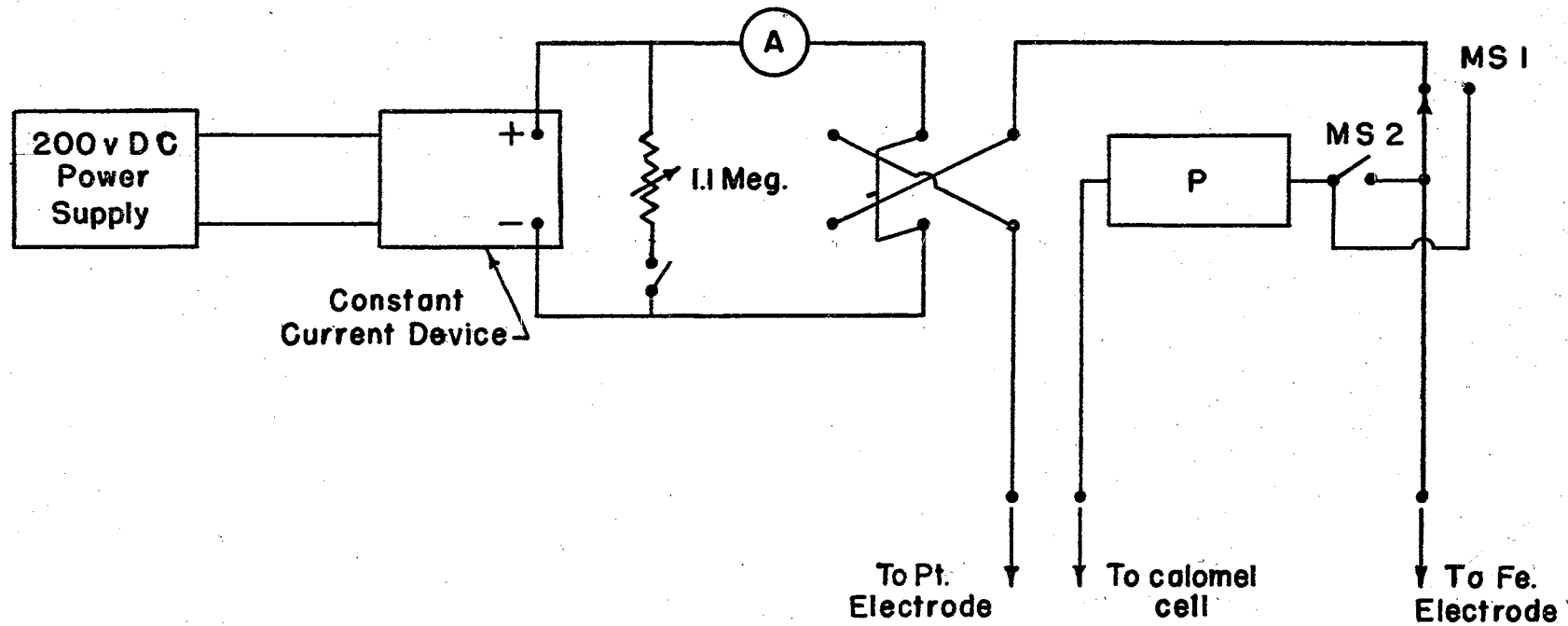


FIGURE 3- Electrical circuit for polarization runs

as well as inter concentration. In all cases, it was expeditious to run the cathodic portion first since the electrode tended to regain the zero current potential it exhibited at the start more quickly than if the electrode were first made an anode.

The potential of the electrode at the various impressed currents was determined by a potentiometric measurement between the electrode and the saturated calomel electrode. Both "open" and "closed" circuit potentials were measured, the former being that potential in which there was no impressed current, in essence the potential of polarization of the electrode, the latter, that potential with current flow. The "closed" circuit potential is a composite reading of polarization potential and IR drop between the two electrodes.

To determine the "closed" circuit potential, micro switch 1 (Figure 3) was depressed throwing in the potentiometer which was then balanced to read the potential. Micro switch 2 in the normally closed position was then depressed opening the circuit and throwing in the potentiometer. The "open" circuit potential was read at that point where the galvanometer needle on the potentiometer showed a decided "kick" in one direction followed by a reversal of direction and a long sweep in that direction denoting depolarization. These readings were more difficult to determine than the corresponding "closed" circuit readings and necessitated quickly flicking switch 2 to find the point of initial deflection without too much depolarization. Since the IR drop shows a linear relationship with current, the "open" circuit potential was corrected by plotting the difference between the "closed" and "open" circuit

potentials against applied current and fitting the best straight line through the points by linear regression. These values were then applied to the "closed" circuit readings to obtain the corrected open circuit readings. Potential measurements were recorded three minutes after each current was impressed to standardize the procedure since potentials in inhibited solutions tended to drift with time.

Upon addition of inhibitor to the cell electrolyte, equilibrium was attained in two hours. Therefore, a complete run which included the control run, inhibitor runs at the specified concentrations and subsequent cleaning took about 24 hours.

The amines tested were aniline, cyclohexylamine, dimethylaminoethanol, ethylamine, morpholine, quinoline, and triethanolamine.

Static Corrosion Testing

Coupon Preparation

Rectangular test coupons, one inch by three inches were cut from 0.025 inch Armco sheet stock. Each strip was abraded with Tri-M-ite W 320-A silicon carbide paper with particular emphasis on feathering of edges, then polished with 2/0 emery paper. The coupons were rubbed lightly with commercial abrasive cleanser, rinsed, then etched in 1:3 by volume $\text{HNO}_3 - \text{H}_2\text{O}$ with gentle agitation for one minute. Upon removal from the solution, the samples were quickly immersed in running water, rubbed with abrasive cleanser, rinsed, then dried in acetone. The dried samples were dessicated for 24 hours before weighing to ± 0.0005 grams.

Cell Assembly and Testing Procedure

Each corrosion cell contained four coupons suspended on glass hooks from a rubber stopper. Through the center of each rubber stopper, a fritted glass stick disperser was mounted, which disperser was surrounded by a glass tube long enough to extend just below the level of the electrolyte in the corrosion cell. When the cell was assembled, it was flushed with CO_2 and subsequently filled by siphoning with 650 milliliters of saturated carbonic acid. Following this, inhibitor to the required concentration was added to the cell and Fe Cl_2 to give 0.01 molar in ferrous ion and the cell connected to the gas manifold as shown in Plate I. The inhibitors tested were aniline, cyclohexylamine, dimethylaminoethanol, ethylamine, morpholine, quinoline and triethanolamine at the 0.01% N and 0.05% N level for 2, 4 and 8 days. One cell containing four coupons for each level was run for each time interval noted. Simultaneously two control cells (containing no inhibitor) were run for each time interval.

Coupon Cleaning

The corroded coupons were rinsed in running tap water, cleaned with abrasive scouring powder and dried in acetone. Subsequently, each was immersed in cleaning solution for 15 minutes to remove corrosion product. The stock cleaning solution was made up by diluting 250 milliliters of concentrated HCl with 500 milliliters of water to which was added 15.27 grams of polyethanol RAD 0515 inhibitor. For cleaning of the coupons, 500 milliliters of the stock cleaning solution was diluted to 2,000 milliliters. Weight loss due to cleaning only (as determined by a non-corroded

blank) was of the order of 1.0 to 1.5 milligrams. Following the HCl pickle, the coupons were rinsed, rubbed lightly with abrasive scouring powder, dried in acetone and dessicated for 24 hours before they were reweighed to determine the weight loss.

CHAPTER III

RESULTS

Polarization Data

Typical current-potential relationships are shown in the semilogarithmic plots of Figures 4 through 11. These graphs illustrate the cathodic and anodic behavior of the iron electrode in four of the seven inhibitors tested. Complete data for all inhibitors are included in Appendix B. The potentials shown are the corrected "open" circuit potentials; the current density is based on 5.0 cm^2 cross sectional area of the iron electrode.

Analysis of the data entailed the determination of the slope of the current-potential curves at regions not far removed from the corrosion potential. When the impressed current is small in comparison with the corrosion current, the current-potential relationship is linear (24). Figures 12 and 13 show typical polarization curves on rectangular coordinates. From curves such as these, the resistance terms r_a and r_c were determined. In the expression

$$r_a = \frac{E_a - E_o}{E_o - E_a} \times \frac{E_o - E_i}{i_e}$$

the slope of the linear portion determines $E_o - E_i/i_e$. For the majority of the control runs, linearity was observed over the whole

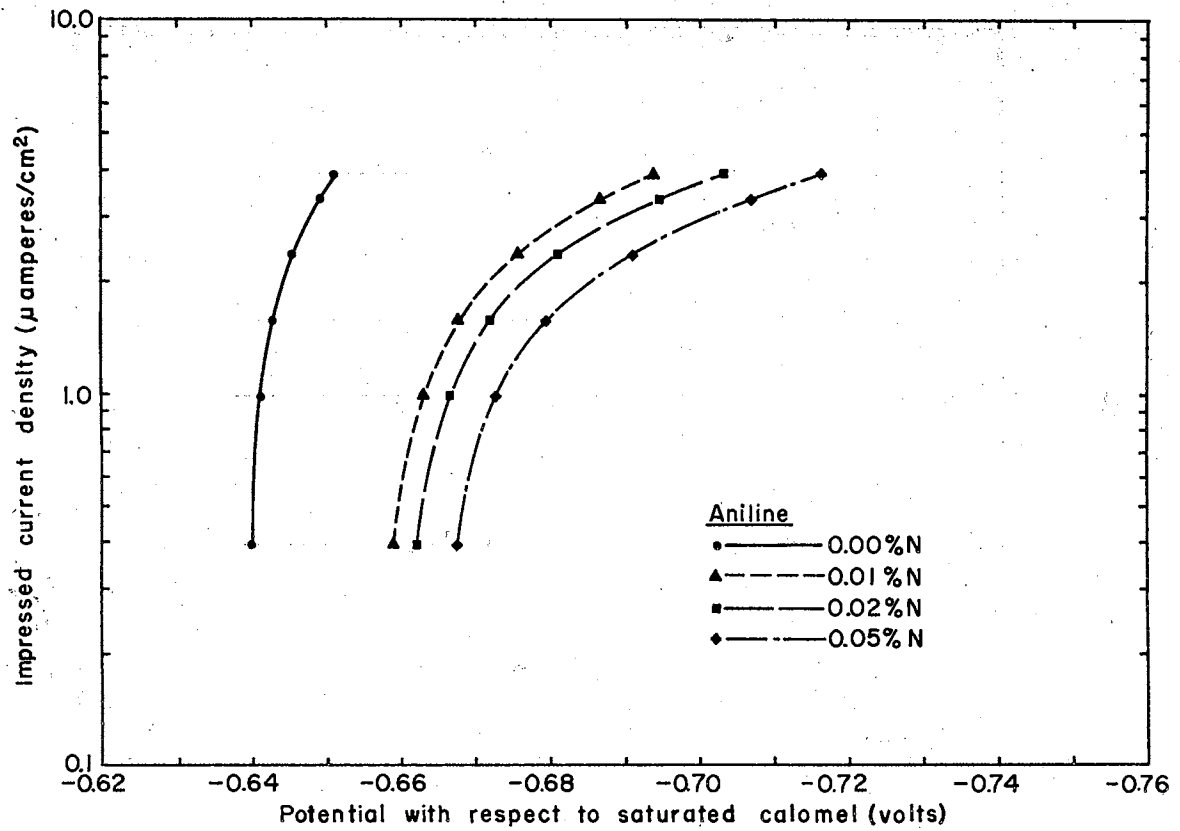


FIGURE 4 - Cathodic polarization of iron electrode

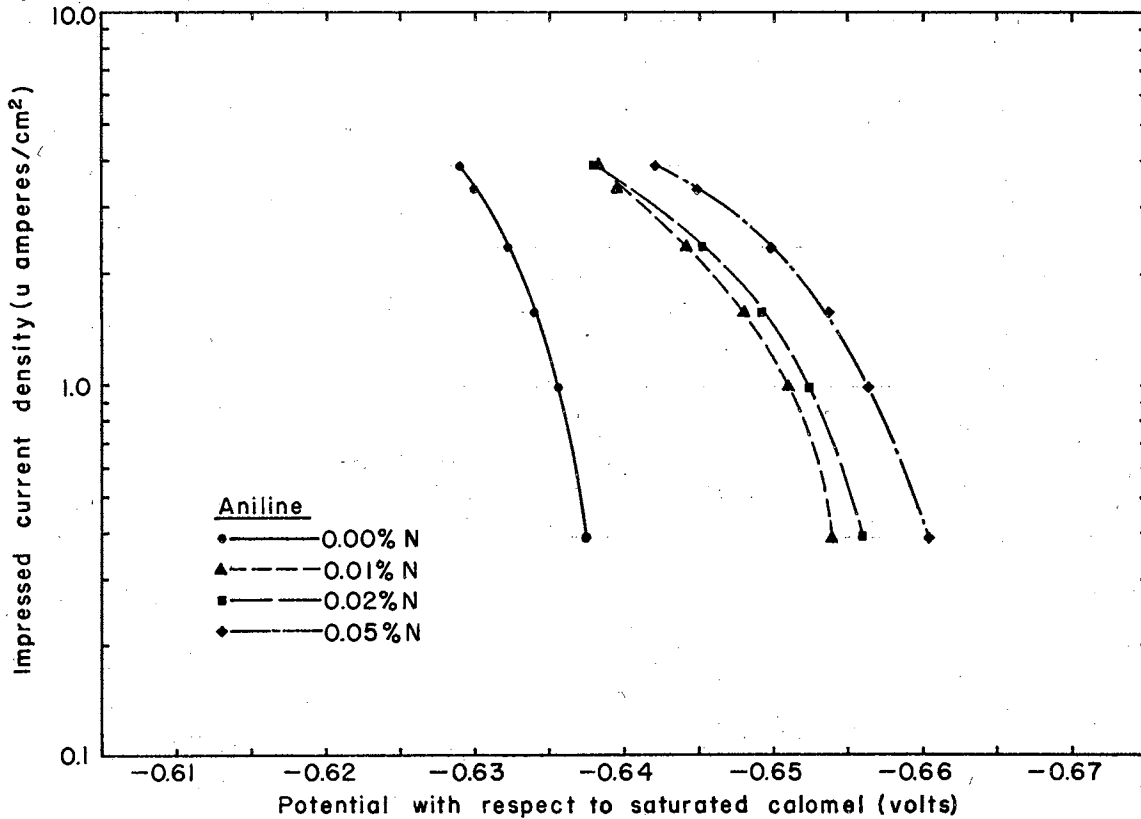


FIGURE 5 - Anodic polarization of iron electrode

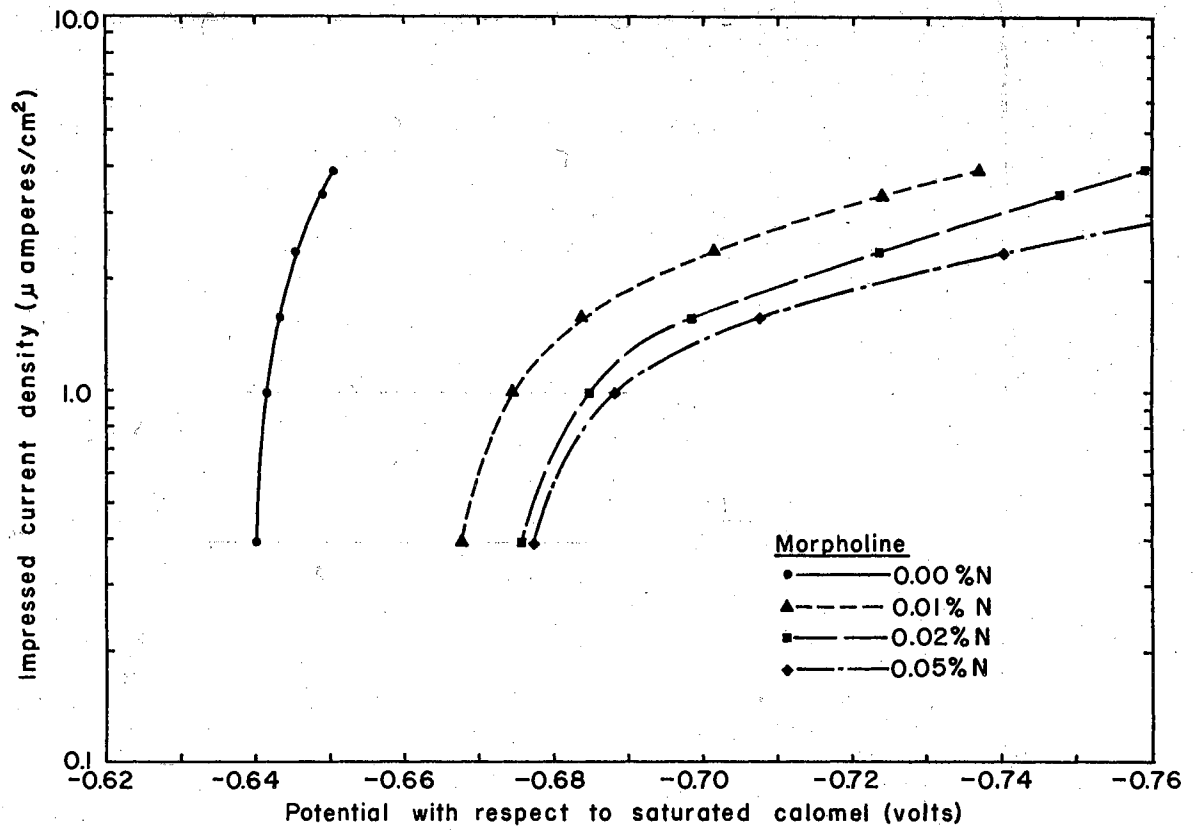


FIGURE 6 - Cathodic polarization of iron electrode

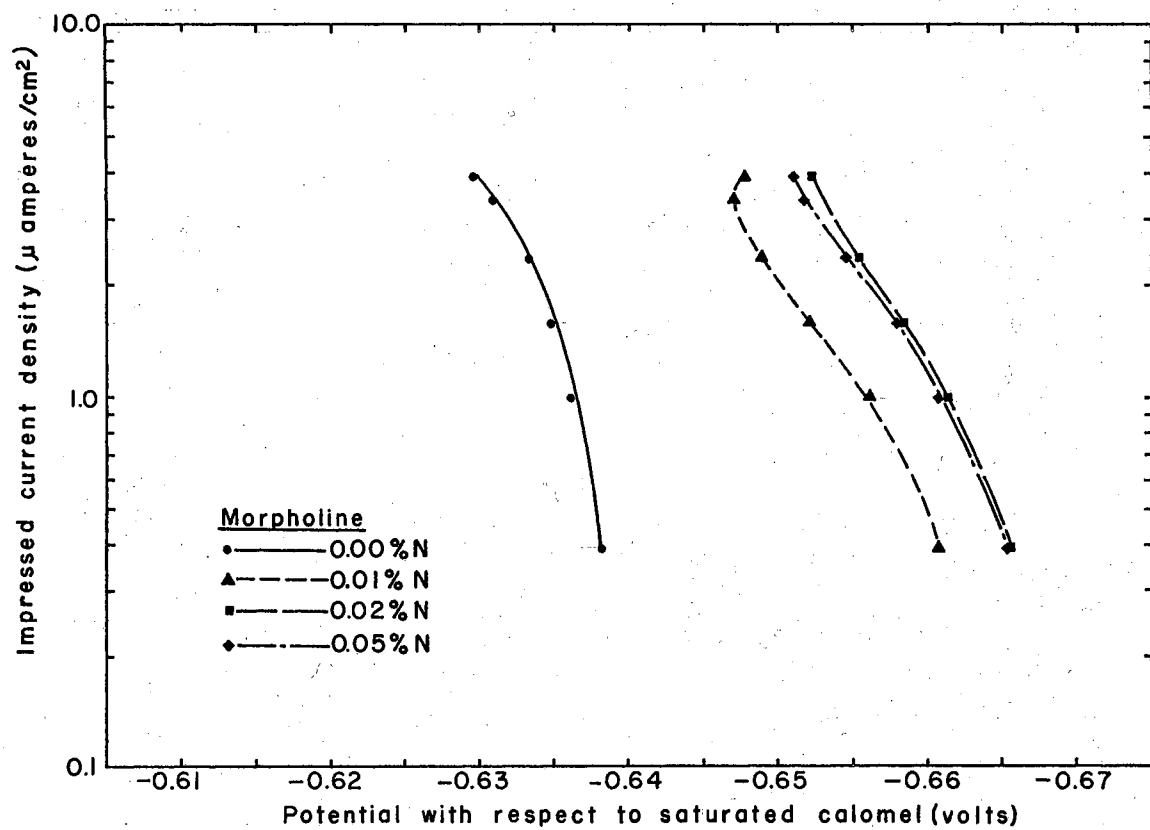


FIGURE 7 - Anodic polarization of iron electrode

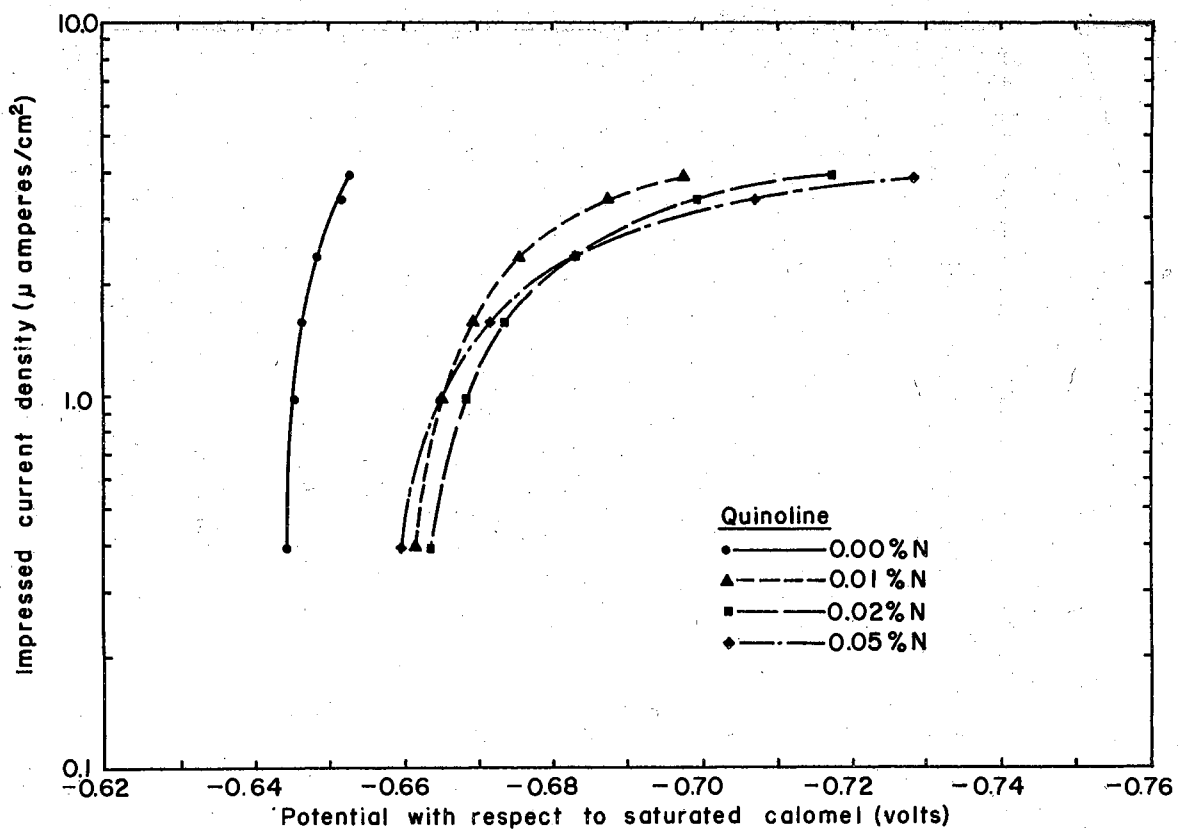


FIGURE 8 - Cathodic polarization of iron electrode

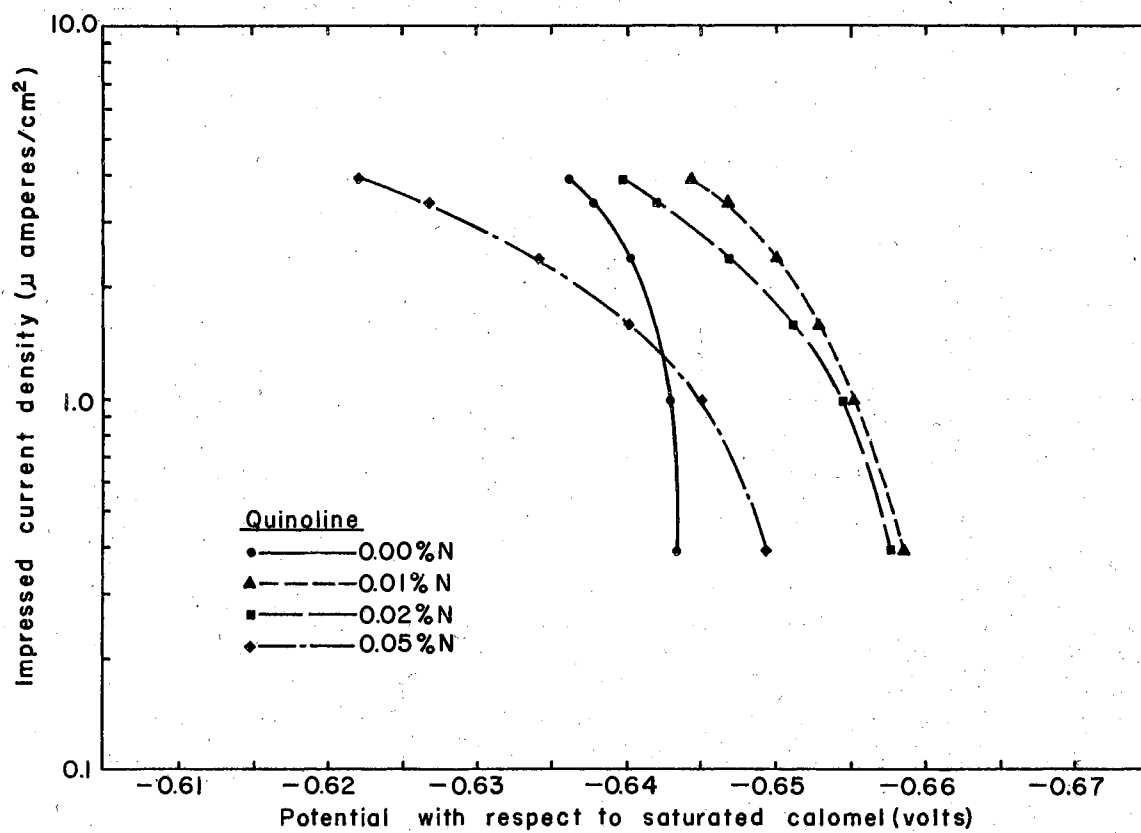


FIGURE 9 - Anodic polarization of iron electrode

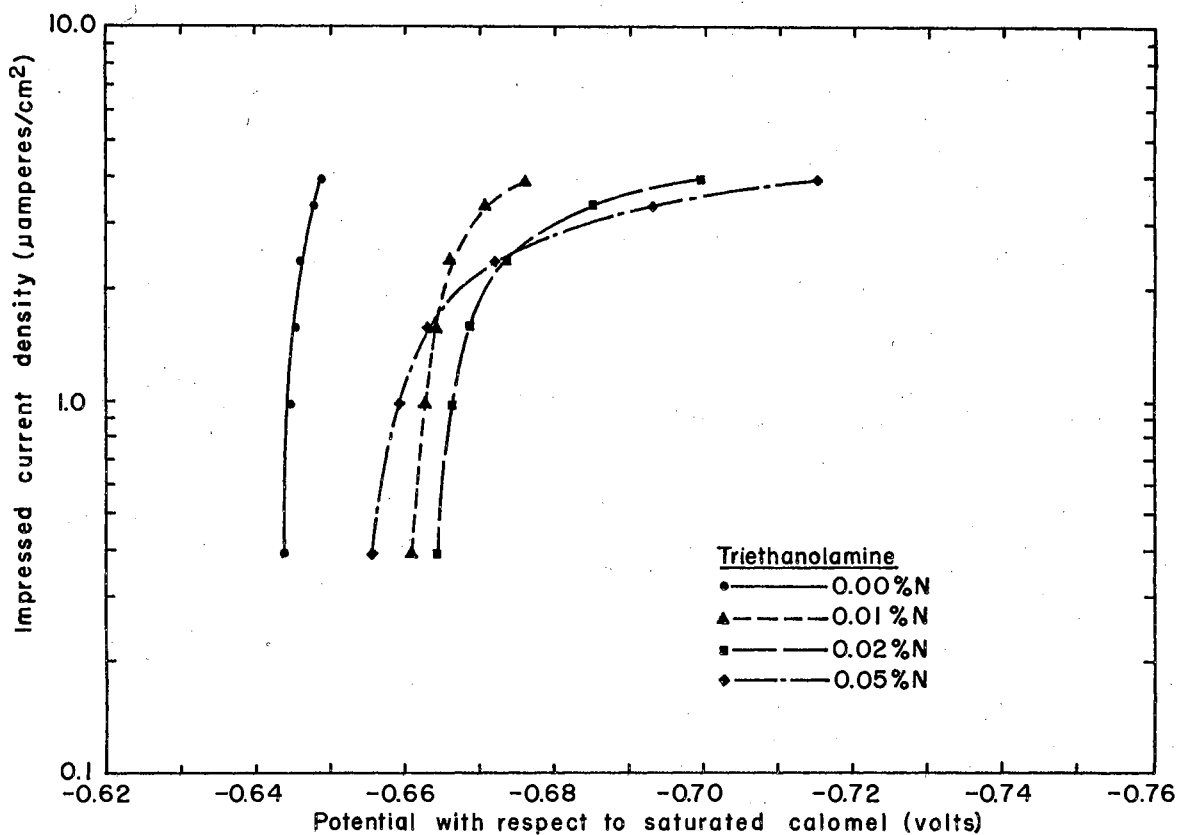


FIGURE 10-Cathodic polarization of iron electrode

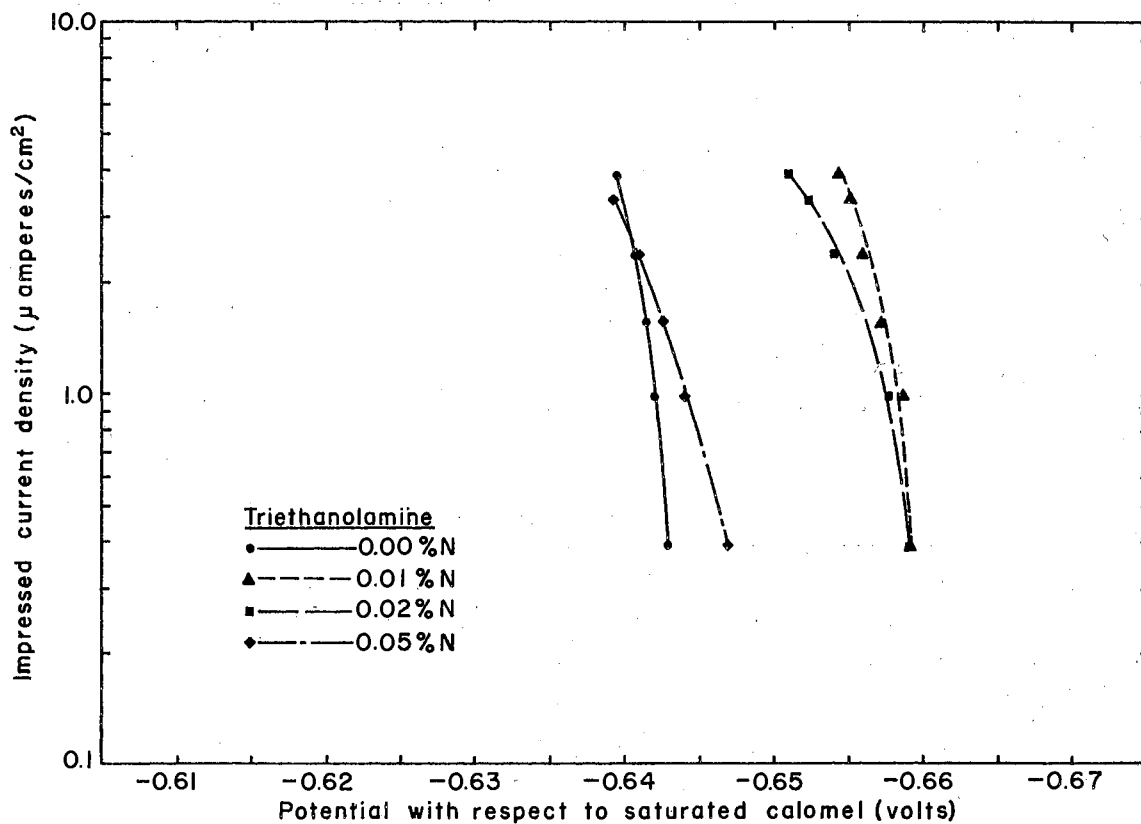


FIGURE 11 - Anodic polarization of iron electrode

range. For inhibited runs, linearity was observed over a limited range of impressed currents, the range depending upon the inhibitor and the concentration. For those curves which show a fairly rapid deviation from linearity straight lines extrapolated to ten micro-amperes were drawn as indicated.

TABLE I

CALCULATED RESISTANCES ON 5.0 CM² ELECTRODE FROM POLARIZATION DATA

Inhibitor	Conc. (%N)	pH	r _a mean (ohm)	r _c mean (ohm)
Aniline	0.00	3.9	338.0	896.5
	0.01	5.0	987.8	1828.3
	0.02	5.1	1214.7	2124.7
	0.05	5.3	1481.1	2122.7
CHXA	0.00	3.9	272.3	664.1
	0.01	5.2	782.5	1394.5
	0.02	5.4	1036.3	1665.9
	0.05	5.7	1448.5	1624.1
DMAE	0.00	3.9	359.6	1086.7
	0.01	5.3	1480.6	3895.6
	0.02	5.6	2162.7	2872.1
	0.05	5.9	3158.0	2746.4
Ethylamine	0.00	3.9	189.6	540.3
	0.01	5.5	747.9	1388.4
	0.02	5.9	967.0	1592.5
	0.05	6.4	1946.5	1894.5
Morpholine	0.00	3.9	323.2	793.1
	0.01	5.3	1603.5	3321.6
	0.02	5.6	2144.2	3602.5
	0.05	5.9	3038.1	3512.1
Quinoline	0.00	3.9	231.2	612.4
	0.01	5.2	636.2	980.3
	0.02	5.2	822.9	1311.8
	0.05	5.5	1971.1	1416.2
TEA	0.00	3.9	151.5	433.9
	0.01	5.4	553.2	952.7
	0.02	5.8	1018.6	1048.4
	0.05	6.1	1936.1	1103.6

CHXA = Cyclohexylamine
 DMAE = Dimethylaminoethanol
 TEA = Triethanolamine

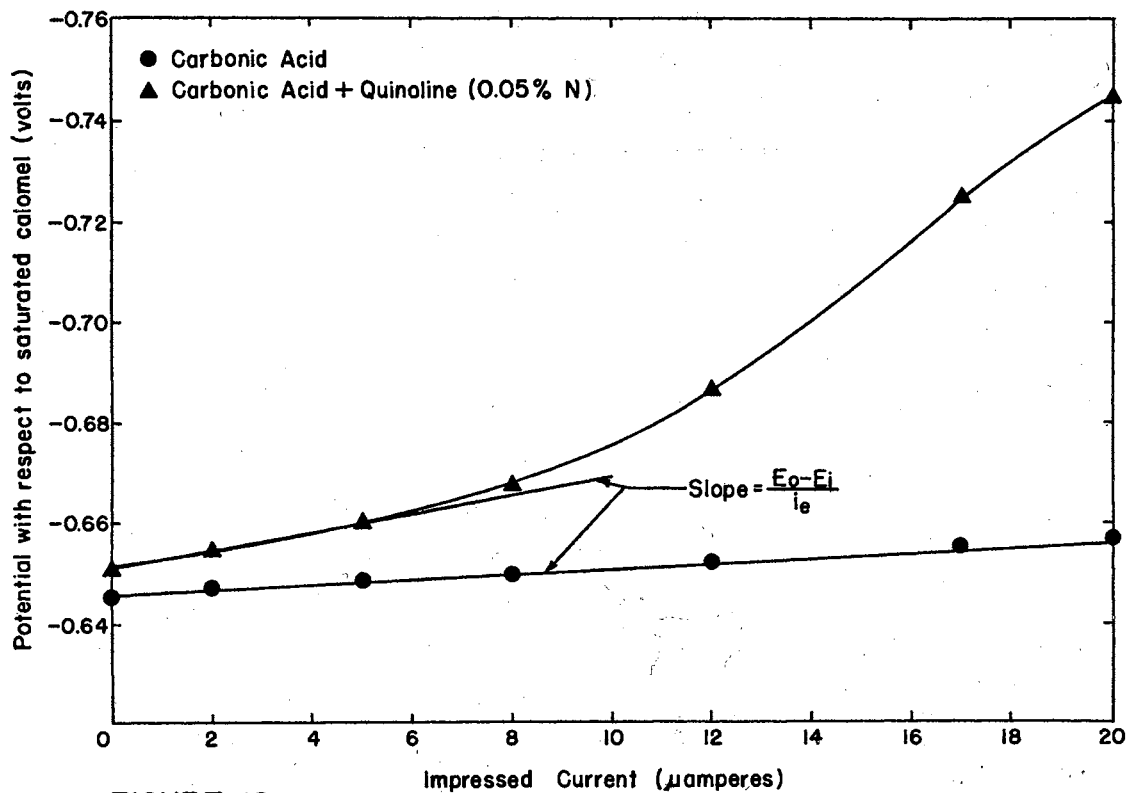


FIGURE 12—Cathodic current-potential relationship for determination of $E_o - E_i / i_e$

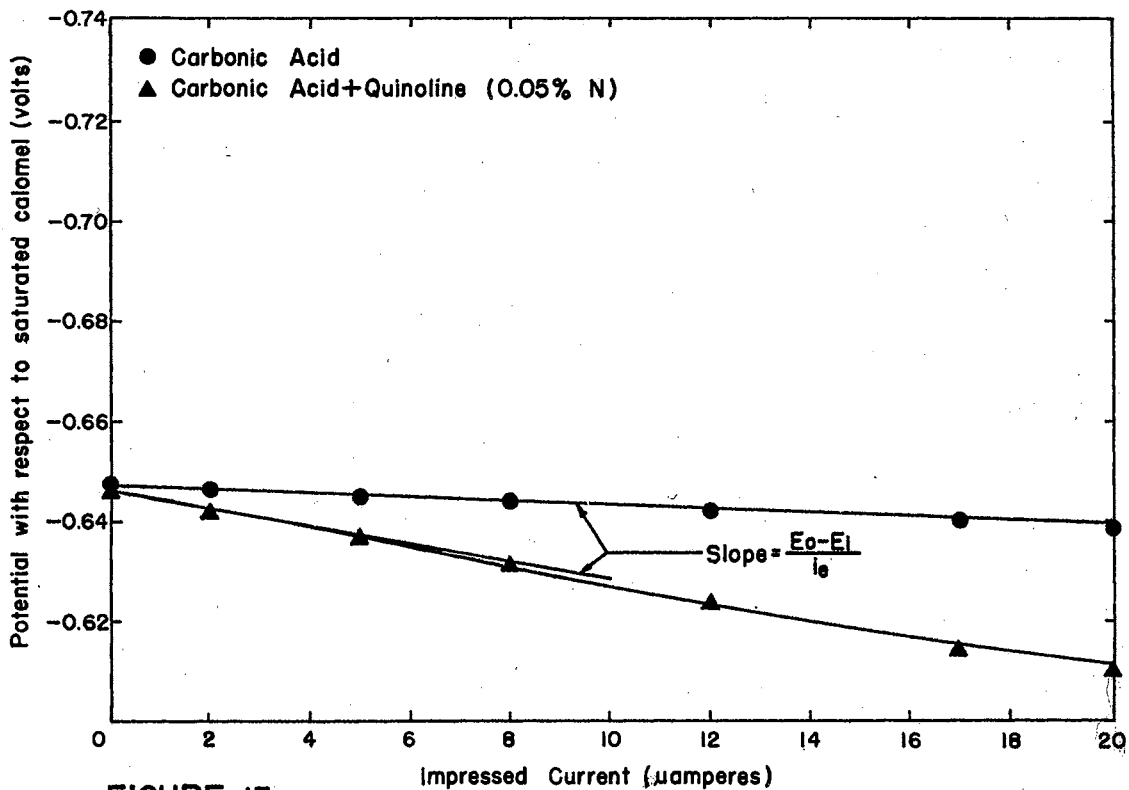


FIGURE 13—Anodic current-potential relationship for determination of $E_o - E_i / i_e$

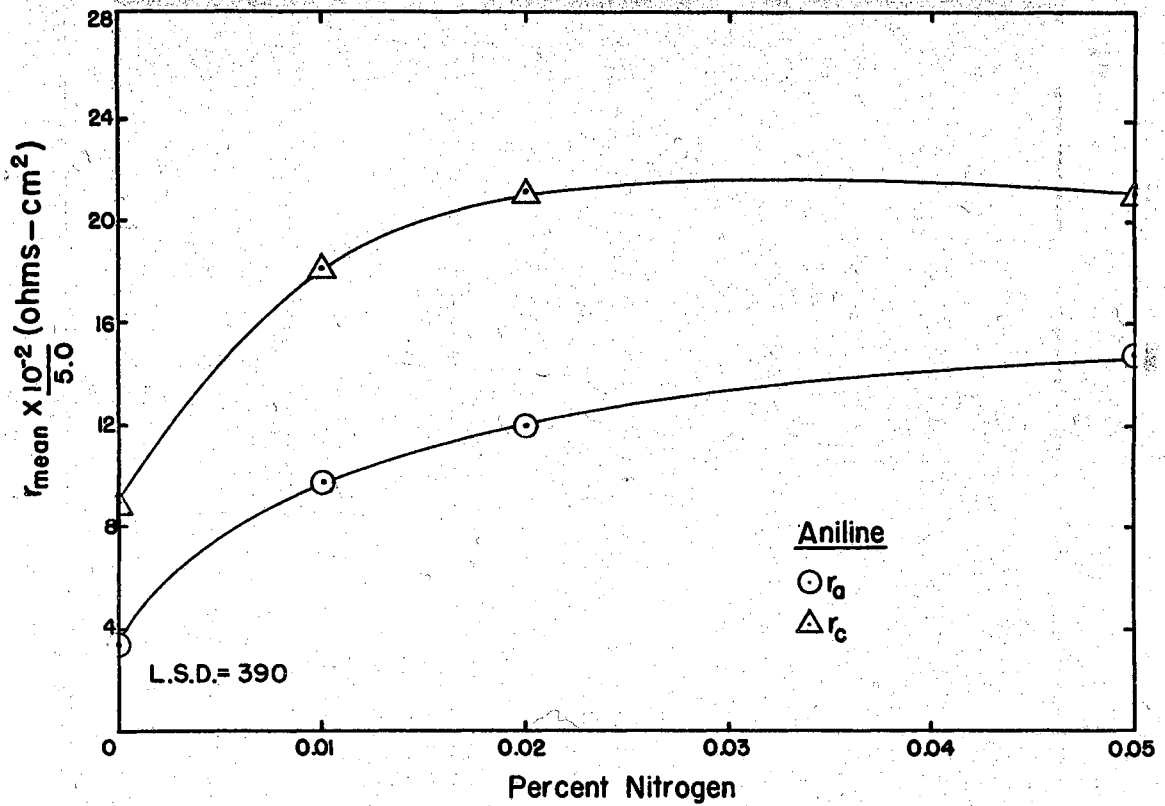


FIGURE 14—Relationship between resistance per unit area and amine concentration

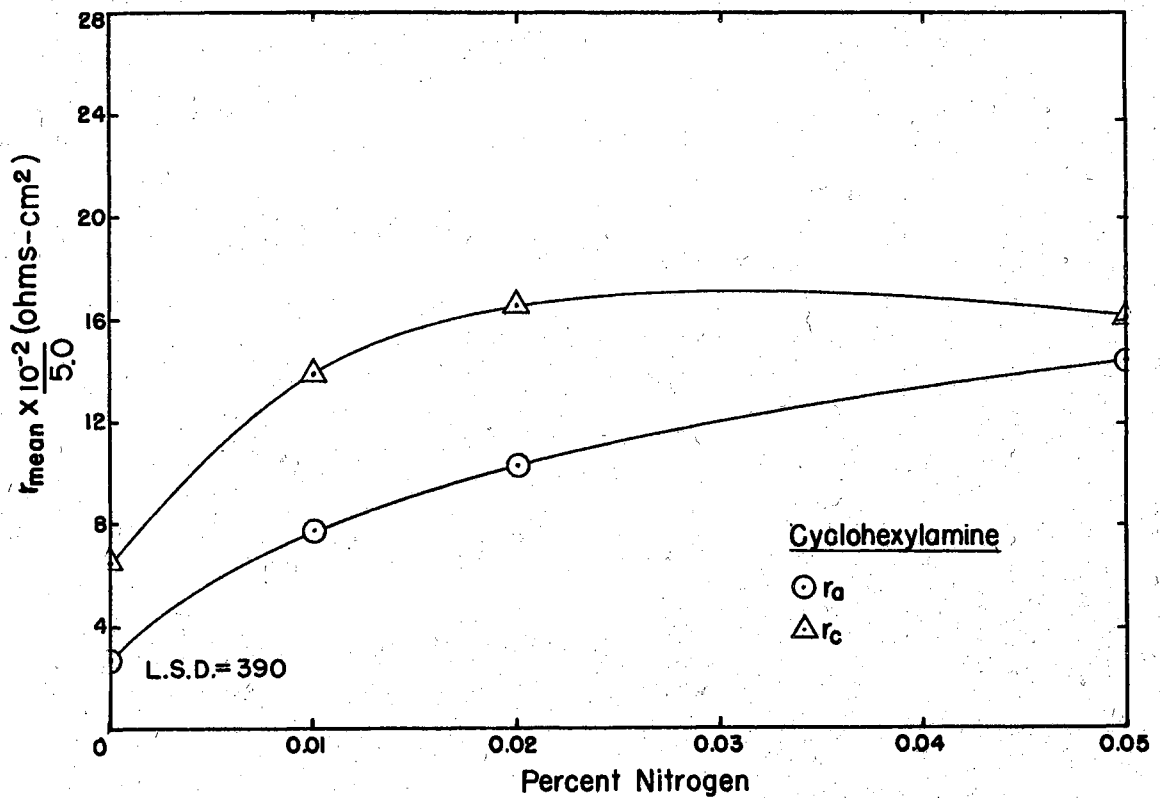


FIGURE 15—Relationship between resistance per unit area and amine concentration

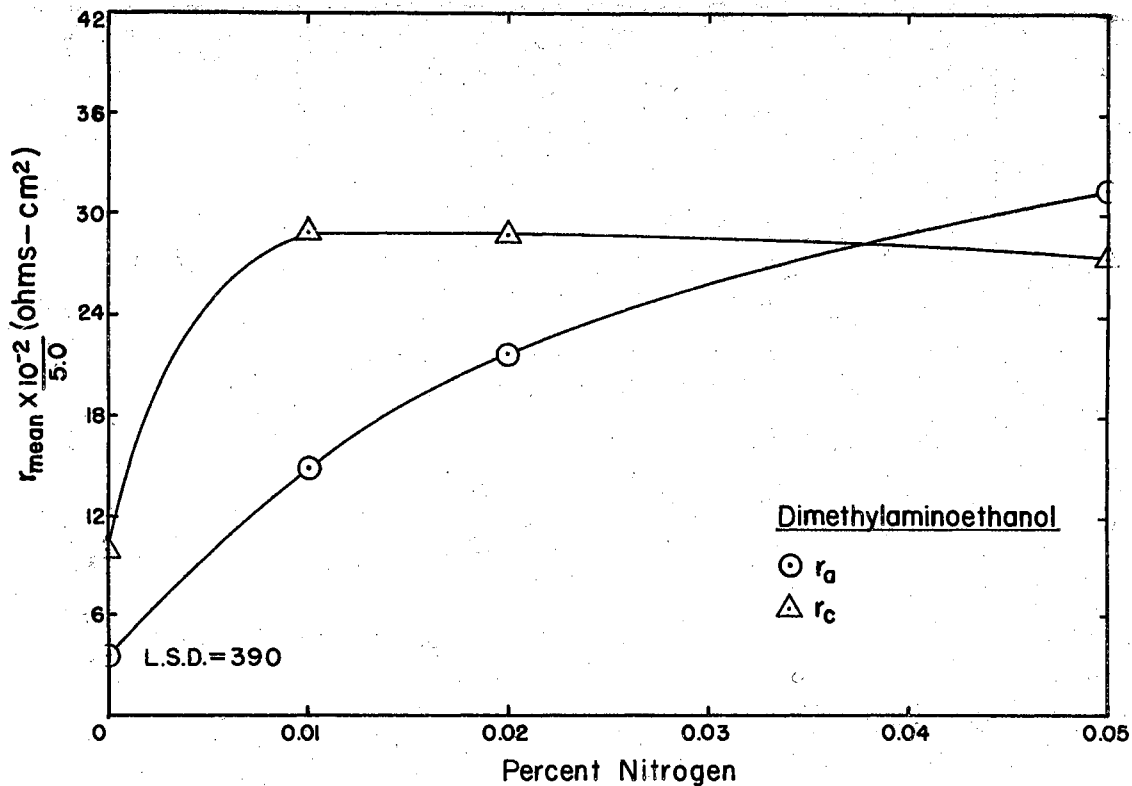


FIGURE 16 - Relationship between resistance per unit area and amine concentration

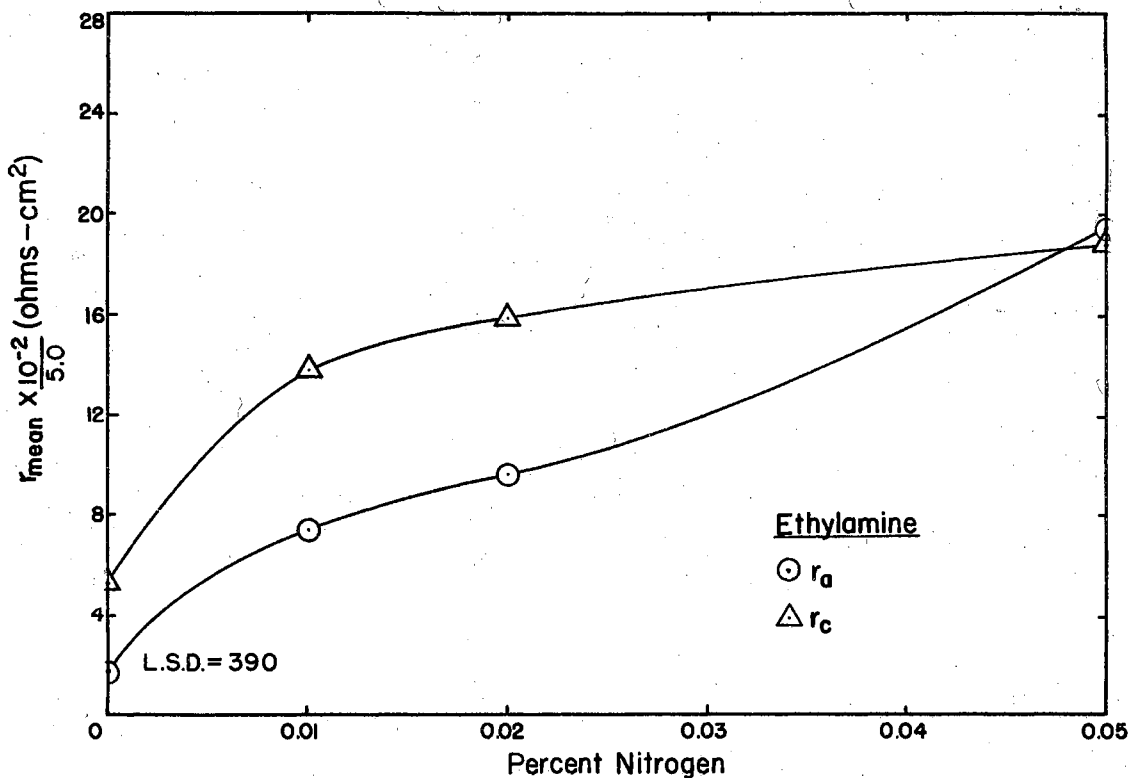


FIGURE 17-Relationship between resistance per unit area and amine concentration

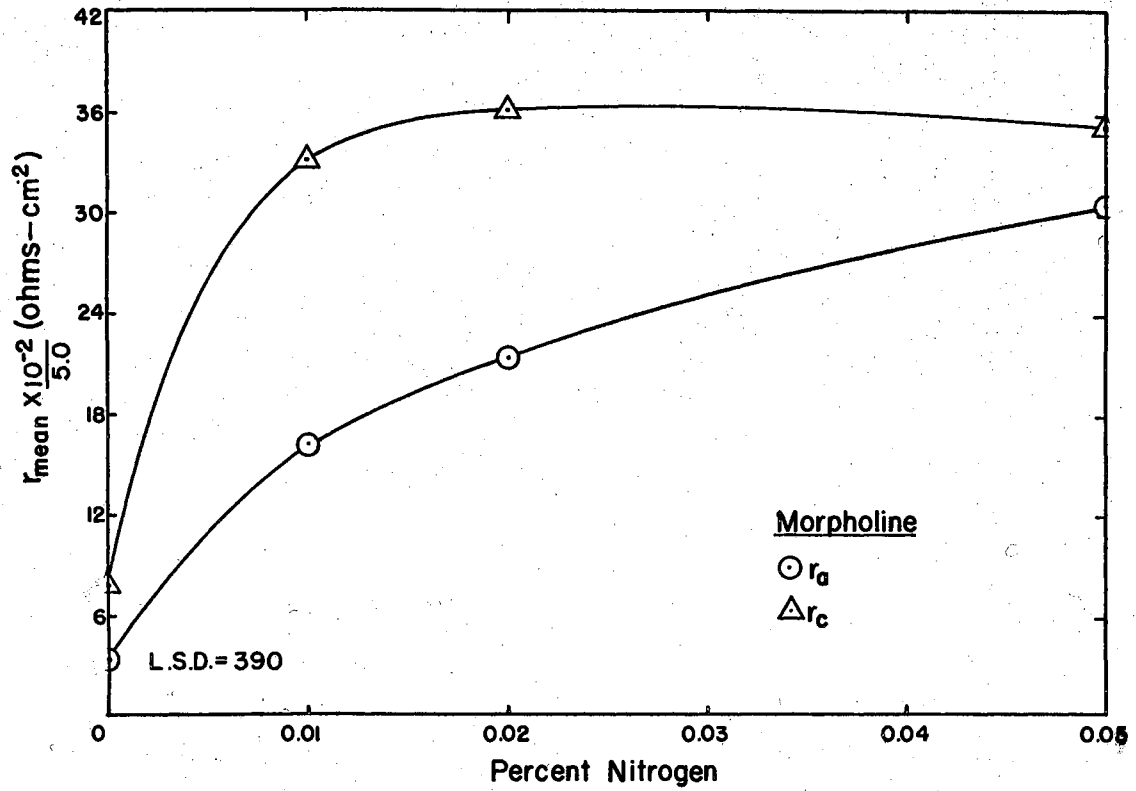


FIGURE 18-Relationship between resistance per unit area and amine concentration

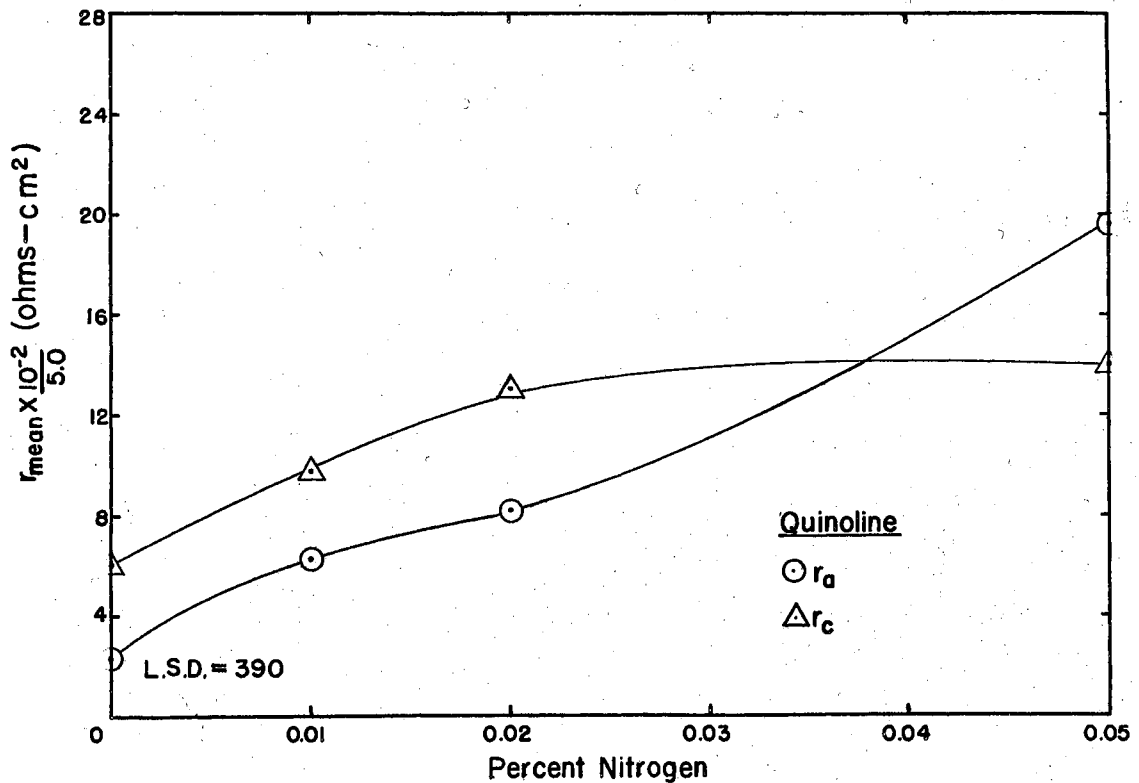


FIGURE 19-Relationship between resistance per unit area and amine concentration

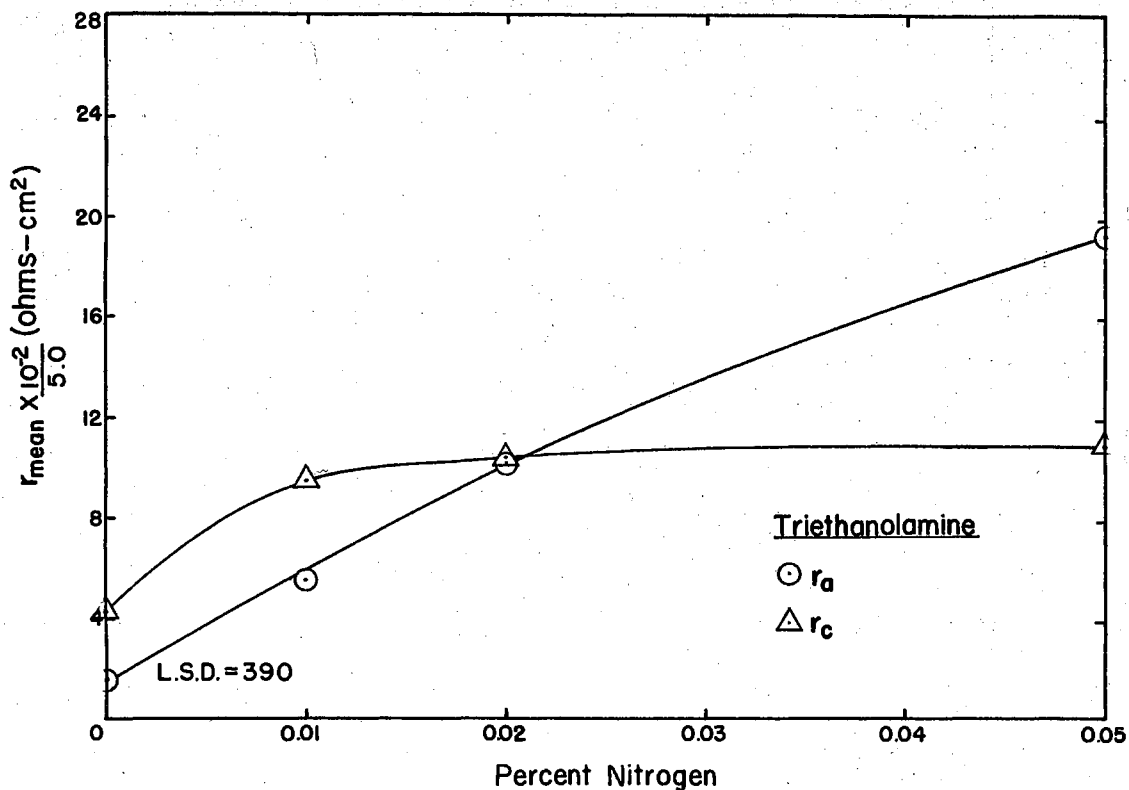


FIGURE 20—Relationship between resistance per unit area and amine concentration

Table I presents the data for r_a mean and r_c mean. These values are the average of individual calculations made on the anodic and cathodic polarization data for each run. At least four runs were made on each inhibitor. Figures 14 through 20 present graphically the data of Table I.

Static Corrosion Tests

Static corrosion test data to determine the relative effectiveness of the amines as inhibitors are shown in Figures 21 and 22. The weight loss per unit area is plotted as a function of time. The values plotted were the average weight loss based on four samples in the same corrosion cell.

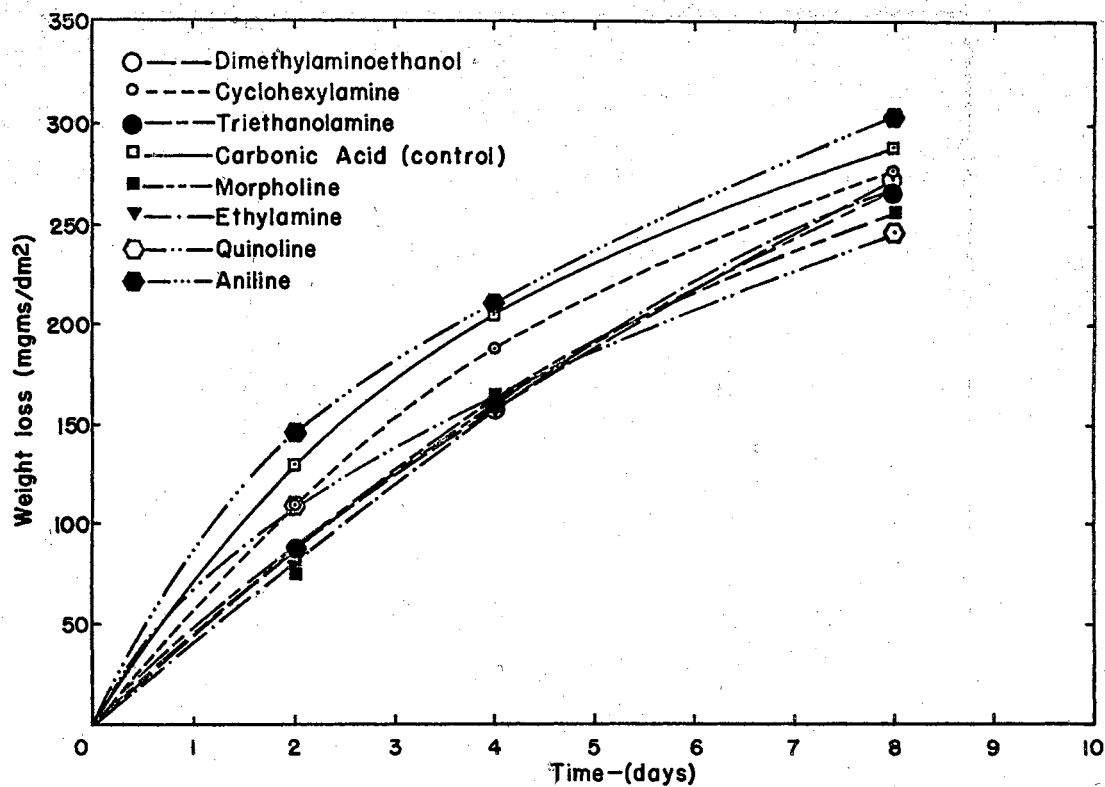


FIGURE 21—Weight loss of samples in inhibited solutions (0.01% N) with time.

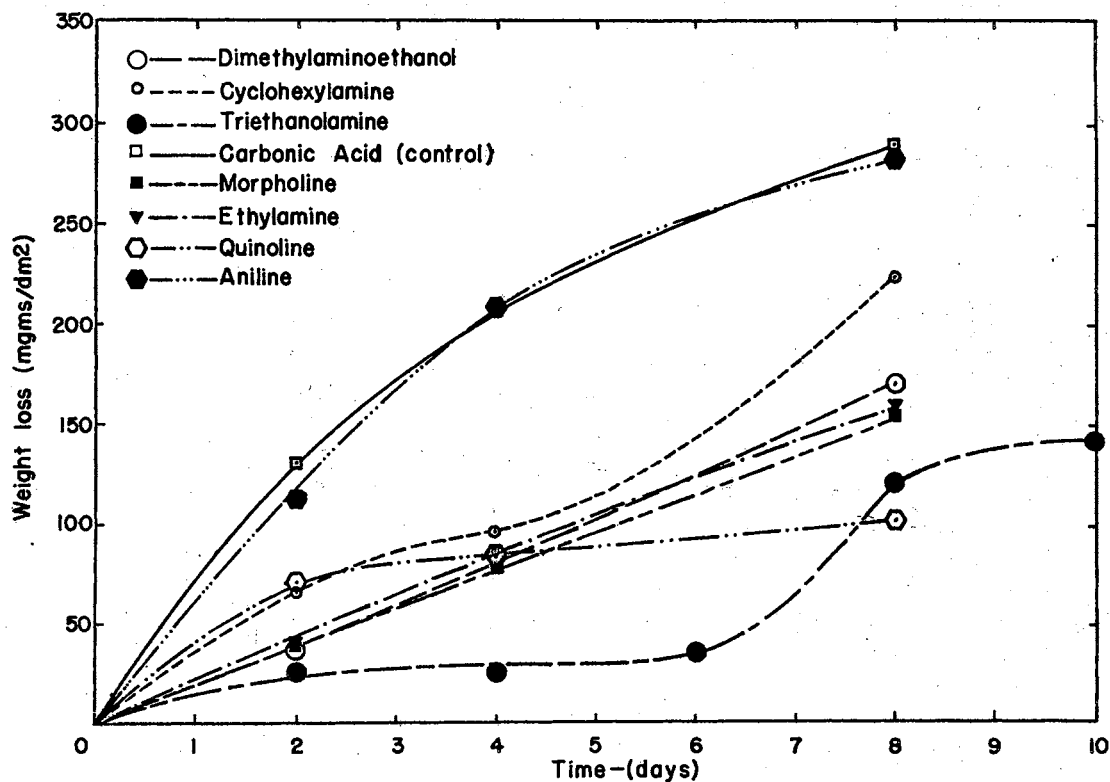


FIGURE 22—Weight loss of samples in inhibited solutions (0.05% N) with time.

CHAPTER IV

INTERPRETATION OF RESULTS

The relationship between the respective resistance terms for anodic and cathodic areas shows that even without inhibitor there is present a calculable resistance. This may be attributed to a "hydride" film, --a monatomic film of chemi-adsorbed hydrogen over the surface (6). The addition of increasing amounts of inhibitor results in an increase in the resistance terms on the respective areas. As illustrated in Figures 14 through 20, the resistance term, r_c , for cathodic areas reaches a maximum at some inhibitor concentration and then levels off or slowly decreases; the resistance term, r_a , for anodic areas although less initially than r_c increases continuously to a greater or lesser degree depending on the inhibitor and in some cases actually crosses that for cathodic areas.

If a comparison is made between triethanolamine and aniline, each shows an increase in r_a and r_c with the addition of inhibitor, with aniline showing higher values for r_c . However, the increase in r_a with increasing inhibitor concentration approaches linearity for triethanolamine, whereas with aniline, increases in r_a and r_c parallel each other with both tending to flatten out at about the 0.02% level. The other inhibitors follow a pattern intermediate between triethanolamine and aniline.

Table II shows the ratio r_a/r_c for the various amines at the four levels of concentration. The rapid rise in r_a/r_c with some of the inhibitors indicates that anodic adsorption is preferential for these. Cathodic adsorption is not precluded since all show a rise in r_c with the addition of inhibitor. Increasing r_a/r_c increases $(A_a/A_c)^2$. When this ratio becomes greater than one the anodic sites will predominate. This appears anomalous in that anodic areas should decrease as inhibitor is adsorbed on these areas. However, to maintain maximum corrosion current as inhibitor is adsorbed larger anodic areas are formed at the expense of cathodic areas.

TABLE II
EFFECT OF CONCENTRATION ON r_a/r_c

<u>Inhibitor</u>	r_a/r_c			
	<u>0.00</u>	<u>0.01</u>	<u>0.02</u>	<u>0.05</u>
Aniline	0.38	0.54	0.57	0.69
CHXA	0.41	0.56	0.62	0.89
DMAE	0.33	0.51	0.75	1.15
Ethylamine	0.35	0.53	0.61	1.03
Morpholine	0.41	0.48	0.60	0.87
Quinoline	0.38	0.65	0.63	1.4
TEA	0.35	0.58	0.97	1.75

With morpholine, preferential cathodic adsorption is manifested in the very high r_c values. In the concentration range tested, the cathodic sites remain predominant. Figure 18 shows that at the 0.05% level r_a is approaching r_c and at some

higher concentration could lie above r_c . This substantiates Hoar's (15) work which showed preferential cathodic adsorption for o-tolylthiourea at low concentrations changing to anodic at higher concentrations. Figure 6, the cathodic polarization curves for morpholine, shows a very marked polarization even at low current densities. This indicates that very little applied current is necessary to make the whole surface function as a cathode for hydrogen evolution. The polarization is such that it is conceivable, even at the current densities employed, the Tafel slope could be determined as outlined by Stern (22). In Figure 7, the corresponding anodic polarization relationships, there is some polarization at lower current densities. However, as the electrode is made increasingly anodic a depolarization is effected as manifested by the tendency for the potential values to be less noble than expected, giving an S shape to the curves. This might indicate some process of desorption of amine if the adsorption were electrostatic.

Figure 10 for triethanolamine shows little cathodic polarization at low current densities. The existence of a relatively high resistance on anodic areas would require a higher current density to make the whole surface a cathode. Triethanolamine shows a marked anodic polarization as evinced by Figure 11.

Aniline shows both anodic and cathodic polarization denoting that this amine is adsorbed on both areas with the ratio of areas remaining essentially constant.

From the relations $r_a/r_c = (A_a/A_c)^2$, $A_a + A_c = 1$ it is possible to calculate the total resistance R offered to the local

corrosion current. The resistance R to local action current is given by:

$$R = r_a/A_a + r_c/A_c \quad (9)$$

Substituting for A_a and A_c in terms of r_a and r_c the resistance is found to be

$$R = r_a + r_c + 2\sqrt{r_a r_c} \quad (10)$$

Previous investigators in their measurements of resistance films by impressed currents have been measuring

$$R = R_a R_c / (R_a + R_c) = \frac{1}{2} \sqrt{r_a r_c}$$

while the effective resistance that limits local action current is actually that given by equation (10). If $r_a = r_c$ then the effective resistance $R = 4\sqrt{r_a r_c}$ which is four times greater than the parallel resistance measured in previous works. This may account for the relatively small increases noted by Rhodes and Kuhn (22).

Table III shows the calculated local action corrosion currents and inhibitor effectiveness based on contributions by resistance film and increased pH. The respective currents tabulated take into account the resistance calculated by equation (10) and are given by: $i_o = (E_c - E_a)/R_o$ where i_o is the local action current with no inhibitor and initial resistance film R_o ; $i_T = (E_c' - E_a)/R_T$ is the current with inhibitor present, E_c' the cathodic potential determined by equation (8) taking into account the increased pH, and R_T the effective total resistance to the current; $i_R = (E_c - E_a)/R_T$ where i_R is the inhibited current if only a resistance film were limiting and there were no increase in pH; $i_{pH} = (E_c' - E_a)/R_o$ where i_{pH} is the inhibited current if only an increase

in pH were effected with no increase over the initial resistance film. The inhibitor effectiveness is calculated as $\frac{i_o - i}{i_o} \times 100$.

TABLE III

CALCULATED CORROSION CURRENTS AND INHIBITOR EFFECTIVENESS

BASED ON RESISTANCE FILM AND pH

Inhibitor	N (%)	Corrosion Current (milliamperes)				Inhibitor Effectiveness (%)		
		i_o	i_T	i_R	i_{pH}	i_T	i_R	i_{pH}
Aniline	0.00	0.115						
	0.01		0.037	0.049	0.087	68	57	24
	0.02		0.030	0.041	0.085	74	64	26
	0.05		0.026	0.038	0.080	77	67	30
CHXA	0.00	0.150						
	0.01		0.045	0.063	0.110	70	58	27
	0.02		0.034	0.050	0.100	77	87	33
	0.05		0.026	0.044	0.091	82	71	39
DIMAÉ	0.00	0.126						
	0.01		0.019	0.028	0.087	25	78	31
	0.02		0.015	0.024	0.079	88	81	37
	0.05		0.012	0.021	0.071	90	83	44
Ethylamine	0.00	0.196						
	0.01		0.043	0.064	0.131	78	67	33
	0.02		0.034	0.053	0.125	83	73	36
	0.05		0.018	0.035	0.100	91	82	48
Morpholine	0.00	0.126						
	0.01		0.019	0.028	0.087	85	78	31
	0.02		0.015	0.024	0.079	88	81	37
	0.05		0.012	0.021	0.071	90	83	44
Quinoline	0.00	0.168						
	0.01		0.060	0.084	0.120	64	50	29
	0.02		0.046	0.064	0.120	73	62	29
	0.05		0.026	0.040	0.110	85	76	35
TEA	0.00	0.244						
	0.01		0.062	0.091	0.167	75	63	32
	0.02		0.038	0.065	0.142	84	73	42
	0.05		0.024	0.045	0.128	90	81	48

A comparison between effectiveness based on i_R and i_{pH} shows that the resistance film is the significant factor in the decrease of corrosion current. Dimethylaminoethanol, morpholine and ethylamine show the greatest effectiveness followed by triethanolamine > quinoline > cyclohexylamine > aniline at the 0.05% level.

No direct correlation can be established between the inhibitor effectiveness as calculated above and that based on static test weight loss data. The data obtained from polarization measurements involved only two hours contact time between the inhibitor and the metal, whereas the shortest static test was over a period of two days. With a mildly corrosive solution like carbonic acid, two hour weight loss tests would be practically meaningless. However, in Figures 21 and 22 the weight losses over the first twenty-four hour period follow generally the same order as that predicted by the calculated inhibitor effectiveness in Table III. The inhibitors at the 0.01% level show very little difference over a period of 8 days (Figure 21). At the 0.05% level, differentiation among inhibitors is marked especially over a period of time. Weight loss data then can predict the permanency of the inhibitor. This cannot be obtained from polarization data unless measurements are made periodically over an extended period.

With a relatively mild acidic electrolyte such as carbonic acid, the addition of the basic amines will increase the pH of the electrolyte. Stern (24) found that the corrosion potential for iron increased by 0.0559 volts per pH unit in the less noble direction. With the addition of inhibitor to the cell, the corrosion potential was increased to less noble values. Table IV shows

the average values for the observed corrosion potentials if the shift were a result of only a rise in pH, E_o'' . It can be seen that the observed corrosion potential is more noble than that calculated indicating that a pH shift is compensated for in varying degrees.

TABLE IV
OBSERVED AND CALCULATED POTENTIALS BASED ON
ADSORPTION AND BASICITY OF INHIBITORS

Inhibitor	N (%)	pH	Δ pH	E_o' (obs) (volts)	E_o'' (pH) (volts)	ΔE^o
						$E_o' - E_o''$ (pH) (volts)
Aniline	0.00	3.9		-0.641		
	0.01	5.0	1.1	-0.657	-0.702	+0.045
	0.02	5.1	1.2	-0.658	-0.708	+0.050
	0.05	5.3	1.4	-0.659	-0.719	+0.060
CHXA	0.00	3.9		-0.640		
	0.01	5.2	1.3	-0.661	-0.713	+0.052
	0.02	5.4	1.5	-0.664	-0.724	+0.060
	0.05	5.7	1.8	-0.663	-0.741	+0.078
DIMAE	0.00	3.9		-0.646		
	0.01	5.3	1.4	-0.666	-0.724	+0.058
	0.02	5.7	1.8	-0.668	-0.747	+0.079
	0.05	6.0	2.1	-0.668	-0.764	+0.096
Ethylamine	0.00	3.9		-0.645		
	0.01	5.5	1.6	-0.666	-0.735	+0.089
	0.02	5.9	2.0	-0.669	-0.757	+0.088
	0.05	6.4	2.5	-0.673	-0.785	+0.112
Morpholine	0.00	3.9		-0.639		
	0.01	5.3	1.4	-0.667	-0.717	+0.050
	0.02	5.6	1.7	-0.671	-0.734	+0.063
	0.05	5.9	2.0	-0.672	-0.751	+0.079
Quinoline	0.00	3.9		-0.641		
	0.01	5.2	1.3	-0.657	-0.714	+0.057
	0.02	5.2	1.3	-0.659	-0.714	+0.055
	0.05	5.5	1.6	-0.651	-0.731	+0.088
TEA	0.00	3.9		-0.644		
	0.01	5.3	1.4	-0.663	-0.722	+0.059
	0.02	5.6	1.7	-0.666	-0.739	+0.073
	0.05	6.05	2.15	-0.660	-0.764	+0.104

In a buffered solution where little or no change in pH would be evident, the corrosion potential would be dependent upon the adsorption characteristics of the inhibitor. Inhibitors which are adsorbed specifically on anodic areas would increase the potential in the noble direction; those adsorbed on cathodic areas in the less noble direction. In a system where both pH and adsorption are operating, the corrosion potential is composite. Then E'_0 is the composite potential of (pH + adsorption), and ΔE_0 , the difference between E'_0 and E''_0 , the potential shift attributable to the adsorption characteristics of the amine.

Hackerman (10) relates the strength of the iron-amine bond in chemisorption to the basic strength of the amine. Figure 23 shows the variation of ΔE_0 with concentration for the inhibitors. The values of ΔE_0 at the 0.05% level decrease in the same order as basic strength, ethylamine > triethanolamine > dimethylaminoethanol > morpholine > cyclohexylamine > quinoline > aniline. This is not the same order as inhibitor effectiveness and, therefore, the potential shift by inhibitors may be a measure only of the bond strength in adsorption.

No statement concerning inhibitor efficiency as a function of size, type or basicity can be made on the limited number of inhibitors tested. Table V summarizes generally the relative order of these factors. Basicity was determined by measurements of the change in pH on the addition of the amine to saturated carbonic acid at 25° C. The relative sizes were estimated on the projected area of Fisher-Hirshfelder-Taylor atomic models. Triethanolamine, dimethylaminoethanol and ethylamine are all pyramidal, but tri-

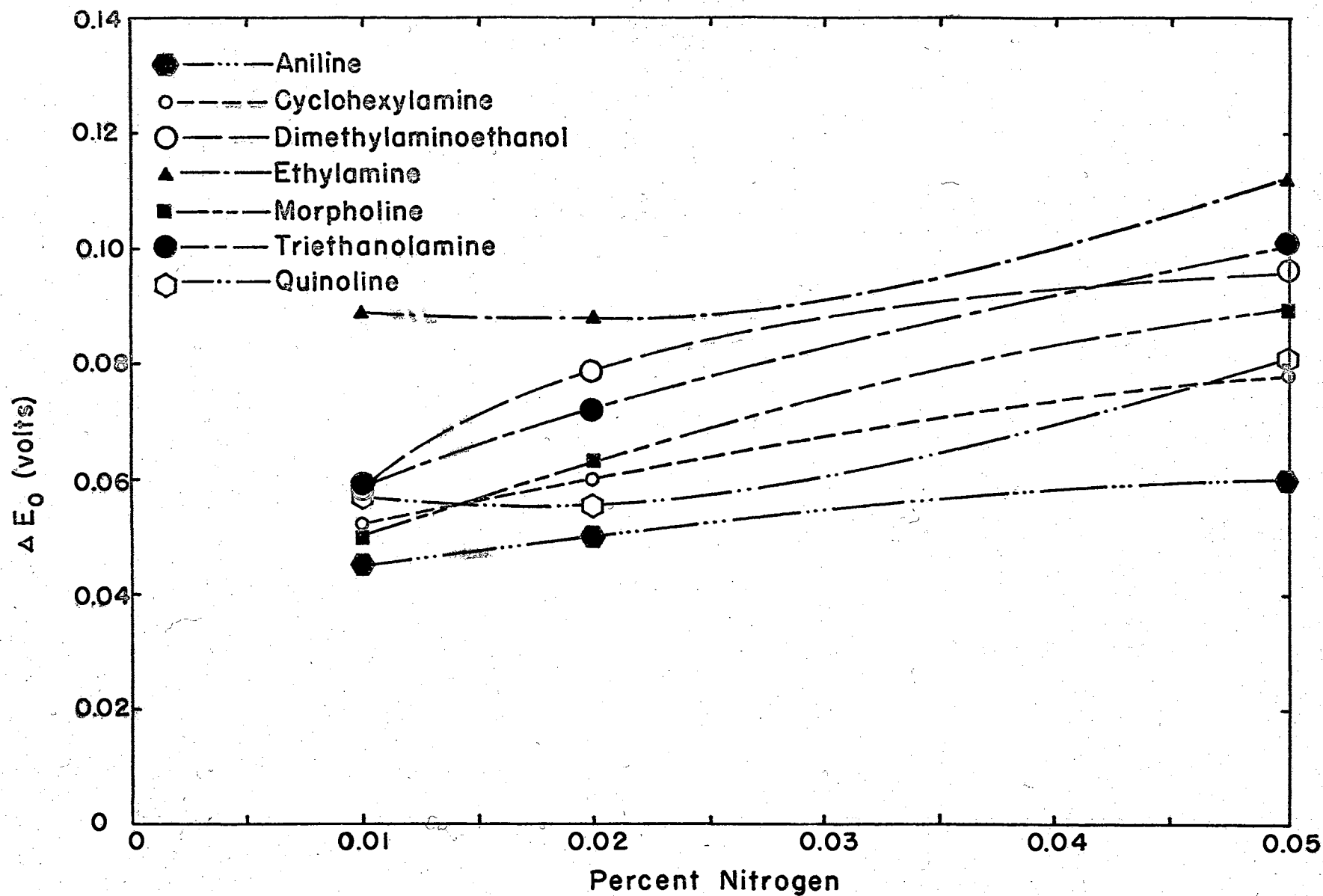
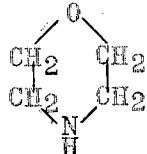
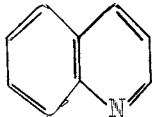
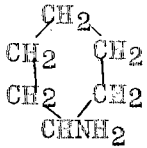
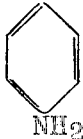


FIGURE 23—Variation of adsorption potential shift with concentration

ethanolamine with its longer chains would cover more area than dimethylaminoethanol which in turn is larger than ethylamine. Mann (19) suggested that the ethyl group in ethylamine is perpendicular to the $-NH_2$ and only slightly tilted and, therefore, the effective area is that covered by $-NH_2$ taken as 25\AA^2 . Similarly the planar ring for aniline was assumed perpendicular to the $-NH_2$ group. Morpholine and cyclohexylamine, since they are saturated cyclic aliphatics, are not planar and therefore, their effective cross sectional area is greater than aniline. Moreover, with nitrogen substituted in the ring, the tendency is to force the ring closer to the metal surface (17) which is the case with quinoline and morpholine.

TABLE V

RELATIVE ORDER OF BASICITY AND SIZE OF THE AMINES ARRANGED
IN DESCENDING ORDER OF INHIBITOR EFFECTIVENESS

Inhibitor Effectiveness	Formula	Type	Basicity	Size
DMAE	$N(CH_3)_2CH_2CH_2OH$	Tert. aliphatic	3	4
Morpholine		Sec. saturated cyclic aliphatic	4	3
Ethylamine	$NH_2CH_2CH_3$	Prim. aliphatic	1	7
TEA	$N(CH_2CH_2OH)_3$	Tert. aliphatic	2	1
Quinoline		Tert. heterocyclic	6	2
CHXA		Prim. saturated cyclic aliphatic	5	5
Aniline		Prim. aromatic	7	6

The three best inhibitors represent the three types of amines tested, none of which is the largest of the group. Generally, however, the tertiary amines are more effective in the corrosion of iron in carbonic acid. Bailar (1) states that, although useful data are limited, iron III coordinates with tertiary amines more readily than with secondary or primary. If chemisorption is complexing of the iron in situ, then the inhibiting properties of the tertiary amines may be explained on this basis.

Tables XX through XXVI in Appendix B contain the analysis of variance (23) for the seven inhibitors. The analyses were made on the average of r_a and r_c calculated from cathodic and anodic polarization curves (Tables XIII through XIX).

Corrosion data are difficult to reproduce especially under mildly corrosive conditions. Nathan (21) who ran statistical analyses on corrosion inhibitor effectiveness data supplied by a number of laboratories working under Group Committee T-1E of the National Association of Corrosion Engineers (NACE) found there were wide variations in the data within each laboratory and among laboratories. He states that: "---even under the most carefully controlled conditions of experimentation wide variations are observed in weight losses, pit frequency, etc.---". For this reason the statistical data are presented here in terms of the standard error of the mean. Confidence limits may then be set at any desired level, and at the discretion of the reader.

The Least Significant Difference (L.S.D.) of 390 as shown on Figures 14 through 20 was calculated from the sum of the squares of the error terms for the inhibitors. This figure is

used as the criterion for the divergence of the respective r_a and r_c values. If the difference between values of r_c and r_a at the same concentration exceeds the L.S.D. then the probability is at least 0.95 that these resistances are different. With this test it is possible to predict the concentration region in which r_a and r_c approach each other or cross, if such is the case.

CHAPTER V

SUMMARY AND CONCLUSIONS

To investigate the mechanism of inhibition by organic amines on the corrosion of iron in mildly corrosive environments, polarization measurements at small impressed current densities were made on an Armco iron electrode in oxygen-free saturated carbonic acid solution at 25° C. Inhibition was interpreted as a film of adsorbed inhibitor on the surface of the metal offering an ohmic resistance to local action current flow. To this end, a mathematical expression was developed to determine the resistance per unit area, r , on anodic and cathodic sites in terms of measurable quantities from polarization data. This development relates the resistance per unit area to the slope of the current-potential curve which is linear at potentials close to the corrosion potential. The total resistance to the corrosion current is the sum of these resistance terms in series. Direct measurement of resistances by impressed currents affords the total resistance as a function of the respective resistance per unit area, in parallel. By the very nature of parallel resistances, only a small increase in total resistance is realized for relatively large increases in either or both resistances per unit area.

The effectiveness of an inhibitor based on the calculated corrosion current as a function of the resistance film depends on

the adsorption characteristics of the amine and the effect on the anodic and cathodic resistances per unit area, and specifically to their ratio, i.e., r_a/r_c . All the amines tested showed increases in both anodic and cathodic resistance terms. However, the inhibitor was effective at that concentration in which r_a/r_c showed a significant increase over this ratio without inhibitor.

The techniques involved in this work are sensitive to contaminants and changes in environment especially traces of inhibitor from preceding runs or the presence of oxygen. However, with reasonable care and further development, the embodying principles could possibly be applied to commercial screening of inhibitors.

Static corrosion tests to determine the stability of the inhibitor effectiveness with time showed that effectiveness was time dependent. Those which showed the best inhibition initially were not necessarily those whose effect was the most lasting. This would serve to indicate that any screening test for inhibitors which does not take into account the permanency of the inhibitor effectiveness is practically valueless unless continuous injection of inhibitor into the system is possible.

To facilitate the characterization of current-potential relationship, polarization measurements in future studies should incorporate an X-Y recorder for definite determination of electrode potentials with impressed current. Equilibrium potentials at specific impressed currents would be definitive using this technique.

Further refinements in technique would require corrosion meter measurements in the cell to determine actual corrosion rates during polarization runs instead of relying upon separate static

corrosion weight loss measurements. Finally, constant monitoring of pH in the cell would define the contribution of concentration overpotential.

Suggestions for Future Work

With the refinements noted, the work should be extended to include commercial inhibitors, long chain amines and organic compounds containing more than one amide group, to correlate size and the availability of more than one ligand per molecule with inhibition. An interesting side issue would lie in the investigation of anionic organic compounds, such as the surfactants, to determine the characteristics of adsorption and the effects on the respective resistances per unit area.

In this research, the polarization at low current density was translated as pure ohmic overpotential, i.e., concentration overpotential and activation overpotential were considered as part of the resistance film. To examine the effect on activation overpotential per se^- , polarization measurements at high current densities should be run to determine the Tafel slopes in the semi-logarithmic region and the principles embodied in the excellent treatment given by Stern applied (24), (25), (26).

BIBLIOGRAPHY

1. Bailar, J. C., - The Chemistry of Coordination Compounds - A.C.S. Monograph, New York, Reinhold Publishing Corporation 1956.
2. Bockris, J. O. M., and Conway, B. E., - "Hydrogen Overpotential and the Partial Inhibition" - Experientia 3, 454 (1947); J. Phys. and Colloid Chem. 53,527(1949).
3. Bruce, J. H., and Hickling, A., - "A Current Stabiliser for Electrolytic Circuits" - J. Scientific Instruments 14,367(1937).
4. Chappell, E. L., Roetheli, B. E., McCarthy, B. Y., - "The Electrochemical Action of Inhibitors in the Acid Solution of Steel and Iron" - Ind. Eng. Chem. 20,582(1928).
5. Elze, J., and Fisher, H., - "The Influence of Inhibitors on the Dissolution of Iron in Acid Solution" - J. Electrochem. Soc. 99,259(1952).
6. Gatty, O., and Spooner, E. C. R., - The Electrode Potential Behaviour of Corroding Metals in Aqueous Solutions - Oxford, Clarendon Press, 1938.
7. Hackerman, N., - "Physical Chemical Aspects of Corrosion Inhibitors" - Corrosion 8,1943(1952).
8. _____ and Cook, E. L., - "Effect of Adsorbed Polar Organic Compounds on Activity of Steel in Acid Solution" - J. Electrochem. Soc. 97, 1(1950).
9. _____ and Cross, B. L., - "Inhibitor Evaluation by the Pearson Null Bridge" - Corrosion 10,407(1954).
10. _____ and George, R. A., - "Acid Corrosion Inhibition by High Molecular Weight Nitrogen Containing Compounds" - Corrosion 11,249(1955).
11. _____ and Makrides, A. C., - "Action of Polar Organic Inhibitors in Acid Dissolution of Metals" - Ind. Eng. Chem. 46,523(1954).
12. _____ and Schmidt, H. R., - "The Role of Adsorption from Solution in Corrosion Inhibitor Action" - Corrosion 5,237(1949).

13. _____ and Sudbury, J. D., - "Effect of Addition of Amines on Electrode Potential of Copper in Buffered Acid Solution" - J. Electrochem. Soc. 93,191(1948).
14. _____, - "Effect of Amines on the Electrode Potential of Mild Steel in Tap Water and Acid Solutions" - J. Electrochem. Soc. 97,109(1950).
15. Hoar, T. P., - "The Action of Organic Inhibitors in the Acid Attack of Mild Steel" - The Pittsburgh International Conference on Surface Reactions, Pittsburgh, Corrosion Publishing Co., 1948.
16. Machu, W., - "The Mechanism and Efficiency of Organic Inhibitors during pickling of Iron" - Trans Electrochem. Soc. 72,333(1937).
17. Mann, C. A., - "Organic Inhibitors of Corrosion" - Trans. Electrochem. Soc. 69,115(1936).
18. _____, Lauer, B. E., and Hulten, C. T., - "Organic Inhibitors of Corrosion - Aliphatic Amines" - Ind. Eng. Chem. 28,159(1936). "Organic Inhibitors of Corrosion - Aromatic Amines" - Ind. Eng. Chem. 28,1048(1936).
19. _____, and Ch'iao, S. J., - "Organic Inhibitors of Corrosion" - Ind. Eng. Chem. 39,910(1947).
20. Muller, W. J., - "The Effect of Cathodic Reactions on the Corrosion of Metals from the Viewpoint of the Local Cell Theory" - Trans. Electrochem. Soc. 76,167(1939).
21. Nathan, C. C., and Eisner, E., - "Statistical Concepts in the Testing of Corrosion Inhibitors" - Corrosion 14,47(1958) *ApriO*
22. Rhodes, F. H., and Kuhn, W. E., - "Inhibitors in the Action of Acid on Steel" - Ind. Eng. Chem. 21,1006(1929).
23. Snedecor, G. W., - "Statistical Methods", 5th ed. Ames, Iowa. The Iowa State College Press, 1956.
24. Stern, M., - "A Method for Determining Corrosion Rates from Polarization Data" - Corrosion 14,60(1958).
25. _____, - "The Electrochemical Behaviour, including Hydrogen Overvoltage, of Iron in Acid Environments" - J. Electrochem. Soc. 102,609(1955).
26. _____, and Geary, A. L., - "Electrochemical Polarization. 1. "A Theoretical Analysis of the Shape of Polarization Curves" - J. Electrochem. Soc. 104,56(1957).

27. Symons, G. E., (Editor), - "Standard Methods for the Examination of Water and Sewage" - 9th ed. New York, American Public Health Assoc., 1946.
28. Tafel, J., - "Polarisation bei Kathodischer Wasserstoffentwicklung" - Z. physik. Chem. 50,641(1904).

APPENDIX A

DERIVATION OF r_a and r_c

Application of Kirchoff's Law to a freely corroding electrode gives (20):

$$E_a + i_L R_a + i_L R_c - E_c = 0 \quad (1)$$

assuming that the only polarization is that for ohmic overvoltage represented by the resistance terms.

$$i_L = \frac{E_c - E_a}{R_a + R_c} = \frac{\Delta E}{\frac{r_a}{A_a} + \frac{r_c}{A_c}} \quad (2)$$

If the total area of the electrode is made up of anodic and cathodic sites only, i.e., there are no insulated spots then:

$$A_a + A_c = 1 \quad (3)$$

and the local action current can be expressed as:

$$i_L = \frac{\Delta E (A_a - A_a^2)}{r_a - A_a (r_a - r_c)} \quad (4)$$

$$\frac{di_L}{dA_a} = \frac{\Delta E (r_a - r_c) \left[(r_a - A_a)(1 - 2A_a) + A_a - A_a^2 \right]}{\left[r_a - A_a (r_a - r_c) \right]^2}$$

For maximum current $\frac{di_L}{dA_a} = 0$

$$\Delta E \left[(r_a - r_c) \left\{ (r_a - A_a)(1 - 2A_a) + A_a - A_a^2 \right\} \right] = 0$$

$$\Delta E \neq 0$$

$$\therefore r_a - 2A_a r_a + A_a^2 r_a - A_a^2 r_c = 0$$

$$r_a (1 - 2A_a + A_a^2) = A_a^2 r_c$$

$$r_a (1 - A_a)^2 = A_a^2 r_c$$

$$r_a / r_c = (A_a / A_c)^2 \quad (5)$$

The potential of a freely corroding electrode is shown as:

$$E_o = E_a + i_L R_a \quad (6)$$

Substituting for i_L from (2)

$$E_o = E_a A_c + E_c A_a \quad (7)$$

When a current i_e is applied to a corroding panel it is impossible

to measure R_a and R_c but:

$$\frac{\Delta E_o}{\Delta I} = R_o = \frac{R_a R_c}{R_a + R_c}$$

for resistances in parallel to the impressed current

$$\therefore R_o = \frac{1}{\frac{1}{r_a} + \frac{1}{r_c}} \quad (8)$$

The potential E_i for impressed current i_e is:

$$E_i = E_o - i_e R_o = E_o - i_e \frac{1}{\frac{1}{r_a} + \frac{1}{r_c}}$$

or:

$$\frac{1}{\frac{1}{r_a} + \frac{1}{r_c}} = \frac{E_o - E_i}{i_e} \quad (9)$$

From (3) and (7) the anodic area A_a and the cathodic

area A_c may be expressed as:

$$A_a = \frac{E_o - E_a}{E_c - E_a} \quad (10)$$

$$A_c = \frac{E_c - E_o}{E_c - E_a} \quad (11)$$

Solution of (5), (9), with substitution from (10) and (11)

yields:

$$r_a = \frac{E_a - E_o}{E_o - E_c} \times \frac{E_o - E_i}{i_e} \quad r_c = \frac{E_o - E_c}{E_a - E_o} \times \frac{E_o - E_i}{i_e}$$

Nomenclature

A_a - area of anodic sites - cm^2

A_c - area of cathodic sites - cm^2

E_a - potential of anodic areas - volts

E_c - potential of cathodic areas - volts

E_i - potential of electrode at impressed current i_e - volts

E_o - corrosion potential of electrode ($i_e = 0$) - volts

R_a - resistance of anodic areas - ohms

R_c - resistance of cathodic areas - ohms

r_a - resistance of anodic areas - $\text{ohm} - \text{cm}^2$

r_c - resistance of cathodic areas - $\text{ohm} - \text{cm}^2$

Proof that i_L has an absolute maximum

$$i_L = \frac{\Delta E}{\frac{r_a}{A_a} + \frac{r_c}{1-A_a}} \quad i_L \geq 0 \quad \text{when } A_a \in (0,1)$$

and i_L is a maximum when

$$y = \frac{r_a}{A_a} + \frac{r_c}{1-A_a} \quad (1)$$

is a minimum. Now:

limit $y = \infty$ so that for some ϵ , where $0 < \epsilon < 1/2$, y will

$A_a \rightarrow 0$ have its absolute minimum on the open interval

$A_a \rightarrow 1$ $(\epsilon, 1-\epsilon)$.

$$\frac{dy}{dA_a} = \frac{-r_a}{(A_a)^2} + \frac{r_c}{(1-A_a)^2} = \frac{-r_a(1-A_a)^2 + r_c(A_a)^2}{(A_a)^2(1-A_a)^2}$$

For an extremum:

$$-r_a(1-A_a)^2 + r_c(A_a)^2 = 0$$

$$(A_a)^2 - (r_a/r_c)(1-A_a)^2 = 0$$

$$\sqrt{A_a + \sqrt{r_a/r_c}(1-A_a)} \sqrt{A_a - \sqrt{r_a/r_c}(1-A_a)} = 0$$

$$\therefore A_a = \frac{-\sqrt{r_a/r_c}}{1 - \sqrt{r_a/r_c}} \quad (2)$$

$$A_a = \frac{\sqrt{r_a/r_c}}{1 + \sqrt{r_a/r_c}} \quad (3)$$

The root shown by (2) lies outside the interval (0,1), therefore

(3) gives the value for the absolute extremum in (1).

$$\frac{d^2y}{dA_a^2} = \frac{2r_a}{(A_a)^3} + \frac{2r_c}{(1-A_a)^3} \quad \text{which is always positive.}$$

Therefore (1) has an absolute minimum at the value of A_a given by (3) and i_L has the corresponding absolute maximum.

Sample Calculations r_a and r_c

Aniline:

Run 51 0.00% Nitrogen

(1) Cathodic run

$$E_o = -0.639 \text{ volts}$$

$$E_a = -0.743 \text{ volts}$$

$$E_c = -0.475 \text{ volts}$$

$$(E_o - E_i)/i_e = 500 \text{ volts /ampere}$$

$$r_a = \frac{E_a - E_o}{E_o - E_c} \times \frac{E_o - E_i}{i_e} = \frac{-0.743 + 0.639}{-0.639 + 0.475} \times 500$$

$$r_a = 317.1 \text{ ohms}$$

$$r_c = \frac{E_o - E_c}{E_a - E_c} \times \frac{E_o - E_i}{i_e} = \frac{-0.639 + 0.475}{-0.743 + 0.639} \times 500$$

$$r_c = 788.5 \text{ ohms}$$

(2) Anodic run

$$E_o = -0.638 \text{ volts}$$

$$E_a = -0.743 \text{ volts}$$

$$E_c = -0.475 \text{ volts}$$

$$(E_o - E_i)/i_e = 500 \text{ volts/ampere}$$

Substituting as shown above

$$r_a = 322.1 \text{ ohms}$$

$$r_c = 776.2 \text{ ohms}$$

APPENDIX B

1. Analysis of Armco Ingot iron

<u>Element</u>	<u>%</u>
Carbon	- 0.012
Manganese	- 0.017
Phosphorus	- 0.005
Sulfur	- 0.025
Silicon	- trace
Iron	- remainder

2. HCl inhibitor for Coupon cleaning in Static Tests -

RAD 0515 - no information on formulation
Hercules Powder Co. Inc.
Wilmington, Delaware.

3. Plastic for encasing electrode -

Armstrong C-7. - two component epoxy resin without
filler.
Armstrong Products Co.,
Argonne Rd.,
Warsaw, Indiana.

TABLE VI
EXPERIMENTAL CURRENT-POTENTIAL RELATIONSHIPS

Aniline

Run #51

Impressed Current (amps.)	Open Circuit Potential (volts)							
	Cathodic				Anodic			
	<u>0.00</u>	<u>0.01</u>	<u>0.02</u>	<u>0.05</u>	<u>0.00</u>	<u>0.01</u>	<u>0.02</u>	<u>0.05</u>
0	-0.639	-0.656	-0.659	-0.664	-0.639	-0.656	-0.659	-0.663
2	0.640	0.659	0.662	0.668	0.638	0.654	0.656	0.660
5	0.641	0.663	0.667	0.673	0.636	0.651	0.653	0.657
8	0.643	0.668	0.672	0.679	0.634	0.648	0.649	0.654
12	0.645	0.676	0.681	0.691	0.633	0.644	0.645	0.650
17	0.649	0.687	0.695	0.707	0.630	0.640	0.640	0.645
20	0.651	0.694	0.703	0.716	0.629	0.638	0.638	0.642

Run #52

Impressed Current (amps.)	Open Circuit Potential (volts)							
	Cathodic				Anodic			
	<u>0.00</u>	<u>0.01</u>	<u>0.02</u>	<u>0.05</u>	<u>0.00</u>	<u>0.01</u>	<u>0.02</u>	<u>0.05</u>
0	-0.639	-0.658	-0.658	-0.657	-0.639	-0.657	-0.658	-0.652
2	0.641	0.660	0.660	0.661	0.638	0.655	0.655	0.648
5	0.642	0.665	0.665	0.667	0.636	0.652	0.651	0.643
8	0.644	0.669	0.671	0.674	0.635	0.650	0.647	0.638
12	0.646	0.676	0.681	0.688	0.633	0.646	0.643	0.633
17	0.649	0.687	0.695	0.707	0.631	0.642	0.638	0.631
20	0.652	0.695	0.704	0.719	0.630	0.641	0.636	0.630

TABLE VI (CONTINUED)

Run #53

<u>Impressed Current</u>	<u>Open Circuit Potential (volts)</u>							
	<u>Cathodic</u>				<u>Anodic</u>			
(μ amps.)	<u>0.00</u>	<u>0.01</u>	<u>0.02</u>	<u>0.05</u>	<u>0.00</u>	<u>0.01</u>	<u>0.02</u>	<u>0.05</u>
0	-0.645	-0.657	-0.658	-0.657	-0.645	-0.657	-0.657	-0.657
2	0.647	0.661	0.662	0.662	0.643	0.653	0.653	0.653
5	0.649	0.667	0.670	0.670	0.641	0.650	0.648	0.647
8	0.652	0.674	0.679	0.681	0.639	0.646	0.644	0.642
12	0.656	0.688	0.697	0.701	0.637	0.642	0.639	0.636
17	0.661	0.709	0.719	0.727	0.633	0.636	0.633	0.629
20	0.665	0.721	0.732	0.738	0.631	0.635	0.629	0.627

Run #54

<u>Impressed Current</u>	<u>Open Circuit Potential (volts)</u>							
	<u>Cathodic</u>				<u>Anodic</u>			
(μ amps.)	<u>0.00</u>	<u>0.01</u>	<u>0.02</u>	<u>0.95</u>	<u>0.00</u>	<u>0.01</u>	<u>0.02</u>	<u>0.05</u>
0	-0.640	-0.657	-0.659	-0.659	-0.640	-0.657	-0.659	-0.659
2	0.640	0.660	0.661	0.662	0.639	0.654	0.656	0.655
5	0.642	0.664	0.666	0.669	0.638	0.651	0.652	0.650
8	0.644	0.669	0.672	0.677	0.636	0.648	0.648	0.645
12	0.646	0.677	0.681	0.693	0.634	0.644	0.644	0.641
17	0.649	0.689	0.695	0.712	0.632	0.637	0.639	0.635
20	0.650	0.697	0.704	0.721	0.631	0.637	0.637	0.632

TABLE VII

EXPERIMENTAL CURRENT-POTENTIAL RELATIONSHIPS

Cyclohexylamine

Run #55

Impressed Current	Open Circuit Potential (volts)							
	Cathodic				Anodic			
(μ amps.)	<u>0.00</u>	<u>0.01</u>	<u>0.02</u>	<u>0.05</u>	<u>0.00</u>	<u>0.01</u>	<u>0.02</u>	<u>0.05</u>
0	-0.638	-0.661	-0.663	-0.662	-0.637	-0.661	-0.663	-0.660
2	0.638	0.664	0.666	0.666	0.637	0.660	0.660	0.658
5	0.639	0.668	0.671	0.673	0.635	0.657	0.657	0.654
8	0.641	0.672	0.677	0.683	0.633	0.655	0.655	0.651
12	0.642	0.681	0.690	0.702	0.633	0.653	0.652	0.648
17	0.645	0.697	0.712	0.732	0.631	0.649	0.648	0.645
20	0.646	0.709	0.730	0.754	0.631	0.647	0.647	0.643

Run #56

Impressed Current	Open Circuit Potential (volts)							
	Cathodic				Anodic			
(μ amps.)	<u>0.00</u>	<u>0.01</u>	<u>0.02</u>	<u>0.05</u>	<u>0.00</u>	<u>0.01</u>	<u>0.02</u>	<u>0.05</u>
0	-0.642	-0.660	-0.663	-0.663	-0.642	-0.660	-0.660	-0.662
2	0.642	0.662	0.666	0.666	0.641	0.658	0.659	0.659
5	0.643	0.666	0.670	0.671	0.640	0.655	0.656	0.655
8	0.645	0.670	0.676	0.677	0.639	0.653	0.654	0.652
12	0.647	0.678	0.688	0.691	0.637	0.651	0.651	0.649
17	0.650	0.695	0.712	0.718	0.635	0.648	0.649	0.646
20	0.651	0.709	0.729	0.739	0.633	0.647	0.648	0.645

TABLE VII (CONTINUED)

Run #58

Impressed Current	Open Circuit Potential (volts)							
	Cathodic				Anodic			
(μ amps.)	<u>0.00</u>	<u>0.01</u>	<u>0.02</u>	<u>0.05</u>	<u>0.00</u>	<u>0.01</u>	<u>0.02</u>	<u>0.05</u>
0	-0.646	-0.665	-0.664	-0.666	-0.646	-0.665	-0.665	-0.666
2	0.647	0.669	0.668	0.670	0.645	0.662	0.660	0.662
5	0.648	0.674	0.676	0.679	0.645	0.658	0.656	0.657
8	0.650	0.681	0.687	0.692	0.643	0.655	0.652	0.654
12	0.651	0.695	0.709	0.717	0.642	0.652	0.650	0.653
17	0.653	0.719	0.742	0.753	0.640	0.649	0.649	0.651
20	0.655	0.734	0.759	0.776	0.639	0.648	0.649	0.650

Run #59

Impressed Current	Open Circuit Potential (volts)							
	Cathodic				Anodic			
(μ amps.)	<u>0.00</u>	<u>0.01</u>	<u>0.02</u>	<u>0.05</u>	<u>0.00</u>	<u>0.01</u>	<u>0.02</u>	<u>0.05</u>
0	-0.639	-0.662	-0.664	-0.663	-0.639	-0.661	-0.664	-0.673
2	0.639	0.663	0.665	0.666	0.638	0.659	0.661	0.671
5	0.640	0.666	0.669	0.670	0.637	0.657	0.658	0.668
8	0.641	0.670	0.673	0.676	0.636	0.655	0.656	0.666
12	0.643	0.676	0.680	0.685	0.635	0.653	0.654	0.664
17	0.645	0.687	0.697	0.704	0.634	0.650	0.653	0.662
20	0.647	0.697	0.711	0.722	0.633	0.649	0.652	0.661

TABLE VII (CONTINUED)

Run #60

Impressed Current	Open Circuit Potential (volts)							
	Cathodic				Anodic			
(μ amps.)	<u>0.00</u>	<u>0.01</u>	<u>0.02</u>	<u>0.05</u>	<u>0.00</u>	<u>0.01</u>	<u>0.02</u>	<u>0.05</u>
0	-0.636	-0.655	-0.662	-0.662	-0.636	-0.655	-0.661	-0.662
2	0.637	0.656	0.664	0.664	0.635	0.652	0.659	0.659
5	0.638	0.659	0.667	0.667	0.634	0.649	0.656	0.657
8	0.639	0.663	0.671	0.672	0.633	0.648	0.654	0.656
12	0.641	0.671	0.679	0.680	0.632	0.645	0.653	0.655
17	0.644	0.686	0.696	0.695	0.630	0.645	0.652	0.654
20	0.646	0.699	0.710	0.710	0.629	0.647	0.652	0.654

Run #61

Impressed Current	Open Circuit Potential (volts)							
	Cathodic				Anodic			
(μ amps.)	<u>0.00</u>	<u>0.01</u>	<u>0.02</u>	<u>0.05</u>	<u>0.00</u>	<u>0.01</u>	<u>0.02</u>	<u>0.05</u>
0	-0.639	-0.665	-0.667	-0.666	-0.639	-0.664	-0.667	-0.667
2	0.639	0.666	0.670	0.668	0.638	0.661	0.663	0.664
5	0.641	0.669	0.674	0.673	0.636	0.659	0.660	0.659
8	0.642	0.673	0.680	0.680	0.635	0.658	0.658	0.656
12	0.643	0.679	0.690	0.692	0.634	0.656	0.656	0.654
17	0.646	0.692	0.709	0.714	0.632	0.654	0.653	0.652
20	0.647	0.701	0.724	0.730	0.631	0.653	0.652	0.653

TABLE VIII

EXPERIMENTAL CURRENT-POTENTIAL RELATIONSHIPS

Dimethylaminoethanol

Run #68

Impressed Current (μ amps.)	Open Circuit Potential (volts)							
	Cathodic				Anodic			
	<u>0.00</u>	<u>0.01</u>	<u>0.02</u>	<u>0.05</u>	<u>0.00</u>	<u>0.01</u>	<u>0.02</u>	<u>0.05</u>
0	-0.646	-0.668	-0.671	-0.672	-0.646	-0.669	-0.641	-0.673
2	0.647	0.672	0.676	0.679	0.645	0.665	0.666	0.666
5	0.649	0.679	0.685	0.691	0.644	0.660	0.660	0.658
8	0.651	0.688	0.698	0.707	0.643	0.656	0.655	0.651
12	0.653	0.702	0.719	0.733	0.640	0.652	0.651	0.646
17	0.656	0.722	0.744	0.764	0.638	0.648	0.647	0.645
20	0.658	0.732	0.756	0.781	0.637	0.647	0.648	0.644

Run #69

Impressed Current (μ amps.)	Open Circuit Potential (volts)							
	Cathodic				Anodic			
	<u>0.00</u>	<u>0.01</u>	<u>0.02</u>	<u>0.05</u>	<u>0.00</u>	<u>0.01</u>	<u>0.02</u>	<u>0.05</u>
0	-0.644	-0.663	-0.665	-0.666	-0.643	-0.665	-0.666	-0.666
2	0.646	0.669	0.671	0.673	0.642	0.659	0.659	0.659
5	0.650	0.680	0.684	0.688	0.639	0.652	0.651	0.649
8	0.654	0.693	0.700	0.706	0.636	0.646	0.645	0.643
12	0.658	0.714	0.725	0.735	0.633	0.641	0.640	0.640
17	0.665	0.738	0.756	0.765	0.630	0.640	0.640	0.640
20	0.668	0.755	0.772	0.787	0.628	0.643	0.643	0.643

TABLE VIII (CONTINUED)

Run #70

<u>Impressed Current</u>	<u>Open Circuit Potential (volts)</u>							
	<u>Cathodic</u>				<u>Anodic</u>			
(μ amps.)	<u>0.00</u>	<u>0.01</u>	<u>0.02</u>	<u>0.05</u>	<u>0.00</u>	<u>0.01</u>	<u>0.02</u>	<u>0.05</u>
0	-0.646	-0.666	-0.666	-0.669	-0.646	-0.666	-0.668	-0.670
2	0.648	0.671	0.672	0.676	0.644	0.662	0.662	0.664
5	0.649	0.680	0.683	0.687	0.642	0.656	0.655	0.656
8	0.652	0.692	0.697	0.702	0.640	0.651	0.649	0.648
12	0.656	0.710	0.718	0.724	0.638	0.646	0.644	0.642
17	0.660	0.734	0.746	0.752	0.634	0.642	0.640	0.641
20	0.664	0.746	0.760	0.770	0.633	0.642	0.641	0.642

Run #74

<u>Impressed Current</u>	<u>Open Circuit Potential (volts)</u>							
	<u>Cathodic</u>				<u>Anodic</u>			
(μ amps.)	<u>0.00</u>	<u>0.01</u>	<u>0.02</u>	<u>0.05</u>	<u>0.00</u>	<u>0.01</u>	<u>0.02</u>	<u>0.05</u>
0	-0.645	-0.668	-0.671	-0.667	-0.646	-0.668	-0.671	-0.669
2	0.645	0.670	0.674	0.671	0.645	0.667	0.668	0.665
5	0.646	0.674	0.678	0.679	0.644	0.664	0.665	0.661
8	0.648	0.679	0.685	0.688	0.643	0.662	0.662	0.657
12	0.649	0.688	0.698	0.710	0.642	0.659	0.659	0.653
17	0.652	0.702	0.720	0.742	0.640	0.656	0.655	0.650
20	0.653	0.713	0.733	0.757	0.640	0.654	0.654	0.648

TABLE IX

EXPERIMENTAL CURRENT-POTENTIAL RELATIONSHIPS

Ethylamine

Run #34

<u>Impressed Current</u>	<u>Open Circuit Potential (volts)</u>							
	<u>Cathodic</u>				<u>Anodic</u>			
(μ amps.)	<u>0.00</u>	<u>0.01</u>	<u>0.02</u>	<u>0.05</u>	<u>0.00</u>	<u>0.01</u>	<u>0.02</u>	<u>0.05</u>
0	-0.653	-0.671	-0.672	-0.680	-0.653	-0.671	-0.672	-0.679
2	0.654	0.673	0.675	0.685	0.652	0.669	0.670	0.675
5	0.654	0.676	0.679	0.694	0.652	0.667	0.667	0.670
8	0.655	0.679	0.683	0.708	0.652	0.665	0.664	0.666
12	0.656	0.685	0.691	0.738	0.651	0.662	0.662	0.663
17	0.657	0.696	0.710	0.765	0.650	0.660	0.659	0.657
20	0.658	0.703	0.720	0.775	0.649	0.658	0.657	0.655

Run #35

<u>Impressed Current</u>	<u>Open Circuit Potential (volts)</u>							
	<u>Cathodic</u>				<u>Anodic</u>			
(μ amps.)	<u>0.00</u>	<u>0.01</u>	<u>0.02</u>	<u>0.05</u>	<u>0.00</u>	<u>0.01</u>	<u>0.02</u>	<u>0.05</u>
0	-0.647	-0.667	-0.672	-0.680	-0.647	-0.667	-0.670	-0.680
2	0.648	0.670	0.674	0.685	0.647	0.667	0.669	0.677
4	0.648	0.672	0.677	0.691	0.646	0.666	0.667	0.674
6	0.649	0.675	0.680	0.698	0.646	0.664	0.665	0.671
8	0.650	0.679	0.686	0.717	0.645	0.662	0.663	0.668
10	0.651	0.688	0.696	0.752	0.644	0.659	0.662	0.664
12	0.651	0.694	0.708	0.765	0.643	0.658	0.661	0.662

TABLE IX (CONTINUED)

Run #72

<u>Impressed Current</u>	<u>Open Circuit Potential (volts)</u>							
	<u>Cathodic</u>				<u>Anodic</u>			
(μ amps.)	<u>0.00</u>	<u>0.01</u>	<u>0.02</u>	<u>0.05</u>	<u>0.00</u>	<u>0.01</u>	<u>0.02</u>	<u>0.05</u>
0	-0.638	-0.661	-0.665	-0.666	-0.638	-0.661	-0.665	-0.667
2	0.637	0.662	0.668	0.670	0.637	0.658	0.662	0.664
5	0.638	0.667	0.676	0.677	0.635	0.655	0.658	0.660
8	0.641	0.675	0.686	0.687	0.634	0.651	0.655	0.658
12	0.643	0.690	0.708	0.708	0.630	0.647	0.651	0.655
17	0.648	0.714	0.739	0.744	0.628	0.646	0.649	0.652
20	0.650	0.729	0.759	0.767	0.627	0.647	0.647	0.652

Run #73

<u>Impressed Current</u>	<u>Open Circuit Potential (volts)</u>							
	<u>Cathodic</u>				<u>Anodic</u>			
(μ amps.)	<u>0.00</u>	<u>0.01</u>	<u>0.02</u>	<u>0.05</u>	<u>0.00</u>	<u>0.01</u>	<u>0.02</u>	<u>0.05</u>
0	-0.643	-0.664	-0.662	-0.667	-0.642	-0.664	-0.667	-0.667
2	0.643	0.667	0.669	0.670	0.641	0.661	0.664	0.664
5	0.645	0.672	0.675	0.677	0.640	0.657	0.660	0.660
8	0.646	0.678	0.683	0.685	0.638	0.654	0.657	0.657
12	0.648	0.690	0.699	0.703	0.636	0.651	0.653	0.653
17	0.651	0.710	0.726	0.735	0.633	0.648	0.650	0.649
20	0.653	0.722	0.740	0.751	0.632	0.647	0.649	0.648

TABLE X
EXPERIMENTAL CURRENT-POTENTIAL RELATIONSHIPS

Morpholine

Run #62

Impressed Current (μ amps.)	Open Circuit Potential (volts)							
	Cathodic				Anodic			
	<u>0.00</u>	<u>0.01</u>	<u>0.02</u>	<u>0.05</u>	<u>0.00</u>	<u>0.01</u>	<u>0.02</u>	<u>0.05</u>
0	-0.639	-0.668	-0.668	-0.667	-0.639	-0.667	-0.666	-0.666
2	0.639	0.674	0.677	0.678	0.637	0.661	0.659	0.658
5	0.641	0.688	0.704	0.718	0.636	0.655	0.653	0.652
8	0.643	0.707	0.732	0.761	0.634	0.652	0.649	0.649
12	0.646	0.733	0.764	0.789	0.632	0.647	0.646	0.648
17	0.648	0.753	0.784	0.812	0.629	0.643	0.645	0.647
20	0.651	0.761	0.792	0.821	0.628	0.644	0.646	0.646

Run #63

Impressed Current (μ amps.)	Open Circuit Potential (volts)							
	Cathodic				Anodic			
	<u>0.00</u>	<u>0.01</u>	<u>0.02</u>	<u>0.05</u>	<u>0.00</u>	<u>0.01</u>	<u>0.02</u>	<u>0.05</u>
0	-0.639	-0.668	-0.672	-0.673	-0.639	-0.668	-0.672	-0.673
2	0.640	0.672	0.677	0.679	0.638	0.664	0.667	0.667
5	0.641	0.680	0.687	0.693	0.637	0.660	0.663	0.662
8	0.642	0.689	0.702	0.715	0.635	0.657	0.659	0.658
12	0.644	0.706	0.725	0.745	0.634	0.652	0.655	0.654
17	0.647	0.724	0.747	0.770	0.632	0.648	0.651	0.651
20	0.650	0.732	0.755	0.781	0.630	0.647	0.651	0.651

TABLE X (CONTINUED)

Run #64

Impressed Current	Open Circuit Potential (volts)							
	<u>Cathodic</u>				<u>Anodic</u>			
(μ amps.)	<u>0.00</u>	<u>0.01</u>	<u>0.02</u>	<u>0.05</u>	<u>0.00</u>	<u>0.01</u>	<u>0.02</u>	<u>0.05</u>
0	-0.638	-0.668	-0.672	-0.673	-0.638	-0.668	-0.672	-0.672
2	0.639	0.673	0.679	0.679	0.637	0.663	0.666	0.666
5	0.641	0.681	0.691	0.691	0.636	0.658	0.661	0.660
8	0.643	0.694	0.713	0.724	0.634	0.655	0.658	0.657
12	0.645	0.715	0.740	0.758	0.632	0.651	0.655	0.654
17	0.649	0.737	0.764	0.785	0.630	0.647	0.651	0.652
20	0.651	0.748	0.772	0.796	0.629	0.648	0.651	0.653

Run #65

Impressed Current	Open Circuit Potential (volts)							
	<u>Cathodic</u>				<u>Anodic</u>			
(μ amps.)	<u>0.00</u>	<u>0.01</u>	<u>0.02</u>	<u>0.05</u>	<u>0.00</u>	<u>0.01</u>	<u>0.02</u>	<u>0.05</u>
0	-0.640	-0.664	-0.671	-0.672	-0.640	-0.665	-0.671	-0.672
2	0.640	0.668	0.676	0.677	0.638	0.661	0.666	0.667
5	0.642	0.675	0.685	0.688	0.637	0.656	0.662	0.662
8	0.644	0.684	0.699	0.708	0.635	0.652	0.659	0.658
12	0.646	0.702	0.724	0.742	0.634	0.649	0.656	0.654
17	0.649	0.725	0.748	0.771	0.631	0.647	0.653	0.652
20	0.651	0.737	0.759	0.784	0.630	0.648	0.652	0.651

TABLE XI

EXPERIMENTAL CURRENT-POTENTIAL RELATIONSHIPS

Quinoline

Run #76

Impressed Current	Open Circuit Potential (volts)							
	Cathodic				Anodic			
(μ amps.)	<u>0.00</u>	<u>0.01</u>	<u>0.02</u>	<u>0.05</u>	<u>0.00</u>	<u>0.01</u>	<u>0.02</u>	<u>0.05</u>
0	-0.646	-0.664	-0.662	-0.651	-0.647	-0.660	-0.658	-0.646
2	0.647	0.665	0.664	0.655	0.646	0.659	0.656	0.642
5	0.649	0.667	0.667	0.661	0.645	0.657	0.652	0.637
8	0.650	0.670	0.671	0.668	0.644	0.655	0.650	0.631
12	0.652	0.675	0.681	0.687	0.642	0.652	0.646	0.624
17	0.655	0.689	0.712	0.725	0.641	0.649	0.642	0.615
20	0.657	0.705	0.729	0.745	0.639	0.648	0.640	0.611

Run #77

Impressed Current	Open Circuit Potential (volts)							
	Cathodic				Anodic			
(μ amps.)	<u>0.00</u>	<u>0.01</u>	<u>0.02</u>	<u>0.05</u>	<u>0.00</u>	<u>0.01</u>	<u>0.02</u>	<u>0.05</u>
0	-0.644	-0.659	-0.661	-0.656	-0.645	-0.660	-0.660	-0.654
2	0.645	0.661	0.663	0.660	0.644	0.659	0.658	0.650
5	0.645	0.665	0.668	0.665	0.643	0.656	0.655	0.645
8	0.646	0.669	0.673	0.671	0.641	0.653	0.651	0.640
12	0.649	0.676	0.683	0.684	0.640	0.650	0.647	0.634
17	0.652	0.688	0.705	0.711	0.638	0.647	0.642	0.627
20	0.653	0.698	0.718	0.728	0.636	0.645	0.640	0.622

TABLE XI (CONTINUED)

Run #78

Impressed Current	Open Circuit Potential (volts)							
	Cathodic				Anodic			
(μ amps.)	<u>0.00</u>	<u>0.01</u>	<u>0.02</u>	<u>0.05</u>	<u>0.00</u>	<u>0.01</u>	<u>0.02</u>	<u>0.05</u>
0	-0.639	-0.655	-0.657	-0.656	-0.639	-0.655	-0.657	-0.647
2	0.640	0.657	0.659	0.658	0.639	0.653	0.655	0.643
5	0.641	0.660	0.664	0.663	0.637	0.651	0.651	0.638
8	0.642	0.664	0.667	0.667	0.637	0.648	0.648	0.633
12	0.644	0.670	0.675	0.675	0.635	0.645	0.645	0.627
17	0.647	0.681	0.690	0.697	0.634	0.641	0.641	0.620
20	0.649	0.692	0.705	0.719	0.632	0.639	0.638	0.618

Run #80

Impressed Current	Open Circuit Potential (volts)							
	Cathodic				Anodic			
(μ amps.)	<u>0.00</u>	<u>0.01</u>	<u>0.02</u>	<u>0.05</u>	<u>0.00</u>	<u>0.01</u>	<u>0.02</u>	<u>0.05</u>
0	-0.633	-0.651	-0.655	-0.642	-0.633	-0.651	-0.654	-0.640
2	0.634	0.653	0.657	0.645	0.633	0.650	0.652	0.637
5	0.634	0.656	0.660	0.651	0.632	0.648	0.649	0.632
8	0.636	0.658	0.663	0.656	0.631	0.645	0.647	0.627
12	0.637	0.663	0.669	0.664	0.630	0.642	0.644	0.622
17	0.639	0.671	0.678	0.679	0.629	0.639	0.639	0.616
20	0.640	0.675	0.686	0.695	0.628	0.637	0.638	0.612

TABLE XII

EXPERIMENTAL CURRENT-POTENTIAL RELATIONSHIPS

Triethanolamine

Run #42

Impressed Current	Open Circuit Potential (volts)							
	Cathodic				Anodic			
(μ amps.)	<u>0.00</u>	<u>0.01</u>	<u>0.02</u>	<u>0.05</u>	<u>0.00</u>	<u>0.01</u>	<u>0.02</u>	<u>0.05</u>
0	-0.643	-0.664	-0.670	-0.674	-0.643	-0.663	-0.669	-0.674
2	0.643	0.666	0.672	0.677	0.642	0.661	0.667	0.671
5	0.644	0.669	0.675	0.684	0.641	0.659	0.664	0.667
8	0.645	0.672	0.680	0.693	0.640	0.655	0.662	0.662
12	0.646	0.680	0.690	0.735	0.639	0.654	0.659	0.658
17	0.647	0.692	0.724	0.785	0.638	0.651	0.655	0.654
20	0.648	0.710	0.745	0.783	0.637	0.650	0.653	0.651

Run #43

Impressed Current	Open Circuit Potential volts)							
	Cathodic				Anodic			
(μ amps.)	<u>0.00</u>	<u>0.01</u>	<u>0.02</u>	<u>0.05</u>	<u>0.00</u>	<u>0.01</u>	<u>0.02</u>	<u>0.05</u>
0	-0.646	-0.666	-0.666	-0.666	-0.646	-0.666	-0.666	-0.666
2	0.647	0.668	0.668	0.670	0.645	0.664	0.663	0.664
5	0.647	0.672	0.671	0.674	0.645	0.661	0.659	0.661
8	0.648	0.676	0.677	0.680	0.644	0.658	0.656	0.658
12	0.649	0.685	0.685	0.690	0.643	0.655	0.652	0.656
17	0.650	0.702	0.709	0.720	0.642	0.652	0.648	0.653
20	0.651	0.712	0.728	0.746	0.641	0.650	0.646	0.652

TABLE XII (CONTINUED)

Run #79

<u>Impressed Current</u> (uamps.)	<u>Open Circuit Potential (volts)</u>							
	<u>Cathodic</u>				<u>Anodic</u>			
	<u>0.00</u>	<u>0.01</u>	<u>0.02</u>	<u>0.05</u>	<u>0.00</u>	<u>0.01</u>	<u>0.02</u>	<u>0.05</u>
0	-0.642	-0.665	-0.665	-0.659	-0.642	-0.665	-0.665	-0.658
2	0.642	0.667	0.668	0.663	0.642	0.663	0.662	0.653
5	0.643	0.670	0.672	0.668	0.641	0.661	0.660	0.650
8	0.644	0.674	0.677	0.676	-0.641	0.659	0.657	0.646
12	0.645	0.680	0.688	0.692	0.640	0.657	0.654	0.642
17	0.646	0.691	0.711	0.730	0.639	0.654	0.651	0.641
20	0.648	0.701	0.727	0.751	0.638	0.652	0.649	0.640

Run #81

<u>Impressed Current</u> (uamps.)	<u>Open Circuit Potential (volts)</u>							
	<u>Cathodic</u>				<u>Anodic</u>			
	<u>0.00</u>	<u>0.01</u>	<u>0.02</u>	<u>0.05</u>	<u>0.00</u>	<u>0.01</u>	<u>0.02</u>	<u>0.05</u>
0	-0.643	-0.660	-0.663	-0.653	-0.643	-0.660	-0.661	-0.649
2	0.644	0.661	0.664	0.656	0.643	0.659	0.659	0.647
5	0.645	0.663	0.666	0.660	0.642	0.658	0.658	0.644
8	0.645	0.664	0.669	0.664	0.641	0.657	0.656	0.643
12	0.646	0.666	0.673	0.672	0.641	0.657	0.654	0.641
17	0.648	0.671	0.685	0.693	0.640	0.655	0.652	0.639
20	0.649	0.676	0.700	0.715	0.640	0.654	0.651	0.640

TABLE XIII

COMPOSITE TABULATION OF DATA FOR CALCULATING RESISTANCES PER UNIT AREA

Aniline

Run #	N (%)	Slope		r_a			r_c			E_a	E_c
		Cathodic (volt/μampere)	Anodic (volt/μampere)	Cathodic (ohms)	Anodic (ohms)	Mean* (ohms)	Cathodic (ohms)	Anodic (ohms)	Mean* (ohms)	(volts)	(volts)
51	0.00	0.00050	0.00050	317.1	322.2	319.6	788.5	776.2	784.2	-0.743	-0.475
	0.01	0.00130	0.00100	970.8	746.8	858.8	1740.8	1339.1	1540.0		-0.540
	0.02	0.00145	0.00120	1068.4	884.2	976.3	1967.9	1628.6	1798.3		-0.545
	0.05	0.00155	0.00130	1144.4	981.1	1062.8	2099.4	1722.5	1911.0		-0.557
52	0.00	0.00050	0.00050	312.1	317.1	314.6	801.0	788.5	794.7		
	0.01	0.00110	0.00110	789.0	821.5	805.3	1533.5	1473.0	1503.3		
	0.02	0.00155	0.00150	1190.2	1128.3	1159.3	2018.6	1994.1	2006.4		
	0.05	0.00185	0.00180	1591.0	1724.2	1657.6	2151.2	1879.1	2015.2		
53	0.00	0.00070	0.00070	403.5	403.5	403.5	1214.3	1214.3	1214.3		
	0.01	0.00185	0.00190	1354.0	1390.6	1372.3	2527.6	2595.9	2561.8		
	0.02	0.00235	0.00200	1804.5	1535.7	1670.1	3060.5	2604.7	2832.6		
	0.05	0.00215	0.00180	1809.4	1514.9	1662.2	2554.7	2138.8	2346.8		
54	0.00	0.00050	0.00050	317.1	312.1	314.6	788.5	801.0	794.8		
	0.01	0.00120	0.00130	878.3	951.5	914.9	1639.5	1776.2	1707.9		
	0.02	0.00140	0.00140	1053.1	1053.1	1053.1	1861.2	1861.2	1861.2		
	0.05	0.00200	0.00170	1683.1	1400.0	1541.6	2376.5	2064.3	2220.4		

* values used for analysis of variance

TABLE XIV

COMPOSITE TABULATION OF DATA FOR CALCULATING RESISTANCES PER UNIT AREA

Cyclohexylamine

Run #	N (%)	Slope		r_a			r_c			$\frac{E_a}{(volts)}$	$\frac{E_c}{(volts)}$	
		Cathodic (volt/ampere)	Anodic (volt/ampere)	Cathodic (ohms)	Anodic (ohms)	Mean*	Cathodic (ohms)	Anodic (ohms)	Mean*			
55	0.00	0.00040	0.00040	257.7	261.7	259.7	621.0	611.3	616.5	-0.743	-0.475	
	0.01	0.00100	0.00080	745.5	596.4	671.0	1341.5	1073.2	1207.4			-0.551
	0.02	0.00130	0.00100	1040.0	818.2	929.1	1625.0	1222.2	1423.6			-0.563
	0.05	0.00180	0.00140	1800.0	1435.0	1617.5	1800.0	1365.9	1583.0			-0.581
56	0.00	0.00050	0.00040	307.2	241.9	274.6	813.0	661.4	737.2			
	0.01	0.00105	0.00095	799.5	738.9	769.2	1378.9	1221.4	1300.2			
	0.02	0.00115	0.00110	920.0	941.2	930.6	1437.5	1285.5	1361.5			
	0.05	0.00150	0.00130	1500.0	1300.0	1400.0	1500.0	1300.0	1400.0			
58	0.00	0.00040	0.00030	253.7	253.7	253.7	630.8	630.8	630.8			
	0.01	0.00160	0.00140	1094.7	978.8	1036.8	2338.5	2002.5	2170.5			
	0.02	0.00215	0.00190	1681.7	1452.9	1567.3	2748.7	2484.6	2616.7			
	0.05	0.00240	0.00200	2174.1	1811.8	1993.0	2649.4	2207.8	2428.6			
59	0.00	0.00040	0.00040	253.7	253.7	253.7	630.8	630.8	630.8			
	0.01	0.00080	0.00090	596.4	670.9	633.7	1073.2	1207.3	1140.3			
	0.02	0.00095	0.00110	760.0	880.0	820.0	1187.5	1375.0	1281.3			
	0.05	0.00135	0.00120	1317.1	913.0	1115.1	1383.8	1577.1	1480.5			

TABLE XIV (CONTINUED)

60	0.00	0.00060	0.00040	411.3	265.8	338.6	875.2	601.9	738.6
	0.01	0.00090	0.00150	777.7	1269.2	1023.5	1041.6	1772.7	1407.2
	0.02	0.00100	0.00120	818.2	1004.1	911.2	1222.2	1434.1	1328.2
	0.05	0.00110	0.00120	1127.5	1200.0	1163.8	1073.2	1200.0	1136.6
61	0.00	0.00040	0.00040	253.6	253.6	253.6	630.8	630.8	630.8
	0.01	0.00070	0.00090	478.9	642.9	560.9	1023.1	1260.0	1141.6
	0.02	0.00150	0.00170	1096.2	1023.1	1059.7	2052.6	1915.8	1984.2
	0.05	0.00140	0.00170	1300.0	1502.3	1401.2	1507.7	1923.7	1715.7

* values used for analysis of variance

TABLE XV

COMPOSITE TABULATION OF DATA FOR CALCULATING RESISTANCES PER UNIT AREA

Dimethylaminoethanol

Run #	N (%)	Slope		r_a			r_c			$\frac{E_a}{E_c}$ (volts)	
		Cathodic (volt/ μ ampere)	Anodic	Cathodic	Anodic	Mean*	Cathodic	Anodic	Mean*		
68	0.00	0.00055	0.00055	312.0	312.0	312.0	969.6	969.6	969.6	-0.743	
	0.01	0.00210	0.00190	1450.9	1255.4	1353.2	3039.5	2875.7	2957.6		-0.557
	0.02	0.00250	0.00230	2050.6	1840.0	1945.3	3047.9	2875.0	2961.5		-0.581
	0.05	0.00320	0.00330	3112.3	3209.6	3161.0	3290.6	3393.0	3341.6		-0.599
69	0.00	0.00095	0.00080	547.6	476.1	511.9	1648.0	1344.0	1496.0		
	0.01	0.00305	0.00290	2301.9	2141.1	2221.5	4041.3	3927.8	3984.6		
	0.02	0.00290	0.00350	2692.9	3250.0	2971.5	3123.1	3769.2	3446.2		
	0.05	0.00370	0.00370	4372.7	4252.2	4312.5	3130.8	3218.5	3175.2		
70	0.00	0.00075	0.00060	425.4	345.9	385.7	1322.2	1040.8	1181.5		
	0.01	0.00250	0.00220	1805.6	1554.1	1679.9	3461.5	3114.3	3287.9		
	0.02	0.00310	0.00290	2808.2	2500.0	2654.1	3422.1	3364.0	3393.1		
	0.05	0.00320	0.00280	3382.9	2960.0	3171.5	3027.0	2648.6	2837.8		
74	0.00	0.00040	0.00040	230.6	226.9	228.8	693.9	705.2	699.6		
	0.01	0.00100	0.00090	702.7	632.4	667.6	1423.1	1280.8	1352.0		
	0.02	0.00130	0.00140	1040.0	1120.0	1080.0	1625.0	1750.0	1687.5		
	0.05	0.00200	0.00160	2235.0	1739.1	1987.1	1789.5	1472.0	1630.8		

* values used for analysis of variance

TABLE XVI

COMPOSITE TABULATION OF DATA FOR CALCULATING RESISTANCES PER UNIT AREA

Ethylamine

Run #	N (%)	Slope		r_a			r_c			$\frac{E_a}{E_c}$ (volts)	
		Cathodic (volt/ μ ampere)	Anodic	Cathodic	Anodic	Mean*	Cathodic	Anodic	Mean*		
34	0.00	0.00025	0.00020	127.5	102.0	114.8	490.3	393.0	441.7	-0.743	-0.475
	0.01	0.00090	0.00070	612.7	476.5	544.6	1322.1	1028.3	1175.2		-0.564
	0.02	0.00125	0.00105	887.5	745.5	816.5	1760.6	1478.9	1619.8		-0.671
	0.05	0.00250	0.00220	2100.0	1902.7	2001.4	2976.1	2543.8	2760.0		-0.679
35	0.00	0.00020	0.00020	108.0	111.6	109.8	370.2	358.3	364.3		
	0.01	0.00080	0.00050	590.3	368.9	479.6	1084.2	677.6	880.9		
	0.02	0.00090	0.00090	639.0	654.5	646.7	1267.6	1237.5	1252.6		
	0.05	0.00200	0.00130	1680.0	1124.3	1402.2	2380.9	1503.1	1942.0		
72	0.00	0.00040	0.00040	261.7	261.7	261.7	611.3	611.3	611.3		
	0.01	0.00080	0.00150	691.7	1268.0	979.9	925.3	1774.4	1349.9		
	0.02	0.00150	0.00150	1258.1	1258.1	1258.1	1788.5	1788.5	1788.5		
	0.05	0.00170	0.00170	2145.9	2083.9	2114.9	1346.8	1386.8	1366.8		
73	0.00	0.00040	0.00050	241.9	302.4	272.2	661.4	826.7	744.1		
	0.01	0.00120	0.00130	948.0	1027.0	987.5	1519.0	1645.6	1582.3		
	0.02	0.00150	0.00130	1228.7	1064.9	1146.8	1831.2	1587.0	1709.1		
	0.05	0.00190	0.00180	2329.0	2206.5	2267.8	1550.0	1468.4	1509.2		

* values used for analysis of variance

TABLE XVII

COMPOSITE TABULATION OF DATA FOR CALCULATING RESISTANCES PER UNIT AREA

Morpholine

Run #	N (%)	Slope		r_a			r_c			$\frac{E_a}{E_c}$ (volts)
		Cathodic (volt/ μ ampere)	Anodic	Cathodic	Anodic	Mean*	Cathodic	Anodic	Mean*	
62	0.00	0.00060	0.00055	386.5	348.8	367.7	931.4	867.3	899.4	-0.743
	0.01	0.00350	0.00280	2418.2	1934.5	2176.4	5065.8	4052.6	4559.2	
	0.02	0.00400	0.00300	3225.8	2600.0	2913.9	4960.0	3461.5	4210.8	
	0.05	0.00450	0.00390	4621.6	4113.7	4367.7	4381.6	3697.4	4039.5	
63	0.00	0.00040	0.00040	253.7	253.7	253.7	630.8	630.8	630.8	
	0.01	0.00195	0.00180	1317.6	1216.2	1266.9	2886.0	2664.0	2775.0	
	0.02	0.00250	0.00250	1829.9	1829.9	1829.9	3415.5	3145.5	3415.5	
	0.05	0.00325	0.00270	2843.8	2362.5	2603.2	3714.3	3085.7	3400.0	
64	0.00	0.00060	0.00050	386.5	322.1	354.3	931.4	776.2	853.8	
	0.01	0.00225	0.00240	1520.3	1621.7	1571.0	3330.0	3552.0	3441.0	
	0.02	0.00315	0.00240	2305.7	1800.0	2052.9	4303.5	3200.0	3751.8	
	0.05	0.00325	0.00310	2768.1	2786.1	2773.0	3815.2	3449.3	3632.3	
65	0.00	0.00050	0.00050	317.1	317.1	317.1	788.5	788.5	788.5	
	0.01	0.00195	0.00180	1471.7	1329.0	1400.4	2583.8	2438.0	2510.9	
	0.02	0.00225	0.00250	1687.5	1875.0	1781.3	3000.0	3333.3	3166.7	
	0.05	0.00285	0.00250	2561.4	2246.8	2404.1	3171.1	2781.7	2976.4	

* values used for analysis of variance

TABLE XVIII

COMPOSITE TABULATION OF DATA FOR CALCULATING RESISTANCES PER UNIT AREA

Quinoline

Run #	N (%)	Slope		r_a			r_c			$\frac{E_a}{(volts)}$	$\frac{E_c}{(volts)}$	
		Cathodic (volt/ampere)	Anodic (volt/ampere)	Cathodic (ohms)	Anodic (ohms)	Mean*	Cathodic (ohms)	Anodic (ohms)	Mean*			
76	0.00	0.00050	0.00040	283.6	223.3	253.5	881.4	716.7	799.7	-0.743	-0.475	
	0.01	0.00070	0.00070	489.4	533.0	511.2	1001.3	919.3	960.3			-0.551
	0.02	0.00090	0.00090	656.6	714.9	685.7	1233.3	1132.9	1183.1			-0.551
	0.05	0.00190	0.00190	2131.7	2393.5	2262.6	1693.5	1508.2	1600.9			-0.569
77	0.00	0.00030	0.00030	172.9	175.7	174.3	520.4	512.1	516.3			
	0.01	0.00100	0.00100	777.8	761.5	769.7	1285.7	1313.3	1299.5			
	0.02	0.00130	0.00110	969.1	837.6	903.4	1743.9	1444.6	1594.3			
	0.05	0.00170	0.00170	1700.0	1780.0	1740.0	1700.0	1623.6	1661.8			
78	0.00	0.00050	0.00040	322.1	253.7	287.9	776.2	630.8	703.5			
	0.01	0.00090	0.00090	761.5	761.5	761.5	1063.6	1063.6	1063.6			
	0.02	0.00120	0.00110	973.6	892.5	933.1	1479.1	1355.8	1417.5			
	0.05	0.00130	0.00170	1300.0	2141.6	1720.8	1300.0	1349.5	1324.8			
80	0.00	0.00030	0.00030	208.9	208.9	208.9	430.9	430.9	430.9			
	0.01	0.00050	0.00060	460.0	552.0	506.0	543.5	652.2	597.9			
	0.02	0.00090	0.00090	761.5	777.7	769.6	1063.6	1041.6	1052.6			
	0.05	0.00155	0.00150	2144.5	2176.1	2160.3	1120.3	1034.0	1077.0			

* values used for analysis of variance

TABLE XIX

COMPOSITE TABULATION OF DATA FOR CALCULATING RESISTANCES PER UNIT AREA

Triethanolamine

Run #	N (%)	Slope		r_a			r_c			$\frac{E_a}{(volts)}$	$\frac{E_c}{(volts)}$	
		Cathodic (volt/ampere)	Anodic (volt/ampere)	Cathodic	Anodic	Mean*	Cathodic	Anodic	Mean*			
42	0.00	0.00025	0.00025	148.8	148.8	148.8	420.0	420.0	420.0	-0.743	-0.475	
	0.01	0.00100	0.00080	759.6	621.4	690.5	1316.5	1030.0	1173.3			-0.560
	0.02	0.00120	0.00080	1082.9	722.0	902.5	1329.7	886.5	1108.1			-0.587
	0.05	0.00165	0.00140	1581.3	1341.7	1461.5	1721.7	1460.9	1591.3			-0.602
43	0.00	0.00025	0.00025	141.8	141.8	141.8	440.7	440.7	440.7			
	0.01	0.00090	0.00090	653.8	653.8	653.8	1239.0	1239.0	1239.0			
	0.02	0.00105	0.00120	1023.4	1169.6	1096.5	1077.3	1231.2	1154.3			
	0.05	0.00160	0.00100	1925.0	1203.1	1564.1	1329.9	831.2	1080.6			
79	0.00	0.00030	0.00025	181.4	151.2	166.3	496.0	413.4	454.7			
	0.01	0.00060	0.00070	455.8	520.0	487.9	789.9	942.3	866.1			
	0.02	0.00130	0.00110	1300.0	1100.0	1200.0	1300.0	1100.0	1200.0			
	0.05	0.00170	0.00180	2505.3	2814.5	2660.0	1153.6	1151.2	1152.4			
81	0.00	0.00030	0.00020	178.6	119.0	148.8	504.0	336.0	420.0			
	0.01	0.00060	0.00030	509.1	251.8	380.5	707.1	357.5	532.3			
	0.02	0.00080	0.00080	864.0	886.5	875.3	740.7	722.0	731.4			
	0.05	0.00120	0.00100	2117.6	2000.0	2058.8	680.0	500.0	590.0			

* values used for analysis of variance

TABLE XX

ANALYSIS OF VARIANCE OF RESISTANCE PER UNIT AREA

1. Anodic sites

Aniline

<u>Source of Variation</u>	<u>Degrees of Freedom</u>	<u>Sum of Squares</u>	<u>Mean Square</u>
Total	15	3,607,542	--
Runs	3	468,304	156,100
Treatment	3	2,862,724	954,232
Error	9	276,514	30,723

Standard Error of Mean = 88

2. Cathodic Sites

Total	15	5,739,400	--
Runs	3	1,348,592	449,530
Treatment	3	4,056,195	1,352,065
Error	9	334,613	38,179

Standard Error of Mean = 96

Least Significant Difference = 390 ($t_{0.05-138}$)

TABLE XXI
ANALYSIS OF VARIANCE OF RESISTANCE PER UNIT AREA

1. Anodic sites

Cyclohexylamine

<u>Source of Variation</u>	<u>Degrees of Freedom</u>	<u>Sum of Squares</u>	<u>Mean Square</u>
Total	23	5,459,081	--
Runs	5	586,239	11,248
Treatment	4	4,357,424	1,089,356
Error	14	515,418	36,816

Standard Error of Mean = 89

2. Cathodic sites

Total	23	7,055,812	--
Runs	5	2,008,977	401,795
Treatment	4	3,880,052	970,013
Error	14	1,166,783	83,342

Standard Error of Mean = 113

Least Significant Difference = 390 ($t_{0.05-138}$)

TABLE XXII

ANALYSIS OF VARIANCE OF RESISTANCE PER UNIT AREA

1. Anodic sites

Dimethylaminoethanol

<u>Source of Variation</u>	<u>Degrees of Freedom</u>	<u>Sum of Squares</u>	<u>Mean Square</u>
Total	15	22,737,182	--
Runs	3	4,766,980	1,588,993
Treatment	3	16,608,875	5,536,292
Error	9	1,361,327	151,259

Standard Error of Mean = 191

2. Cathodic sites

Total	15	17,122,510	--
Runs	3	6,440,423	2,146,786
Treatment	3	9,252,720	3,084,209
Error	9	1,429,367	158,815

Standard Error of Mean = 198

Least Significant Difference = 390 ($t_{0.05-138}$)

TABLE XXIII
ANALYSIS OF VARIANCE OF RESISTANCE PER UNIT AREA

1. Anodic sites

Ethylamine

<u>Source of Variation</u>	<u>Degrees of Freedom</u>	<u>Sum of Squares</u>	<u>Mean Square</u>
Total	15	7,368,962	--
Runs	3	717,800	239,264
Treatment	3	6,447,251	2,149,062
Error	9	203,911	22,656

Standard Error of Mean = 89

2. Cathodic sites

Total	15	5,765,914	--
Runs	3	329,068	109,688
Treatment	3	4,069,883	1,356,614
Error	9	1,366,963	151,882

Standard Error of Mean = 192

Least Significant Difference = 390 ($t_{0.05-138}$)

TABLE XXIV
ANALYSIS OF VARIANCE OF RESISTANCE PER UNIT AREA

1. Anodic sites

Morpholine

<u>Source of Variation</u>	<u>Degrees of Freedom</u>	<u>Sum of Squares</u>	<u>Mean Square</u>
Total	15	19,217,020	--
Runs	3	2,574,468	858,147
Treatment	3	15,464,928	5,154,924
Error	9	1,177,624	130,844

Standard Error of Mean = 180

2. Cathodic sites

Total	15	25,767,230	--
Runs	3	2,638,690	879,555
Treatment	3	22,019,170	7,339,650
Error	9	1,109,370	123,261

Standard Error of Mean = 175

Least Significant Difference = 390 ($t_{0.05-138}$)

TABLE XXV
ANALYSIS OF VARIANCE OF RESISTANCE PER UNIT AREA

1. Anodic sites

Quinoline

<u>Source of Variation</u>	<u>Degrees of Freedom</u>	<u>Sum of Squares</u>	<u>Mean Square</u>
Total	15	7,023,973	--
Runs	3	2,542	843
Treatment	3	6,673,315	2,224,416
Error	9	348,116	38,679

Standard Error of Mean = 98

2. Cathodic sites

Total	15	2,314,161	--
Runs	3	500,178	166,724
Treatment	3	1,580,575	526,853
Error	9	233,408	25,934

Standard Error of Mean = 79

Least Significant Difference = 390 ($t_{0.05-138}$)

TABLE XXVI
ANALYSIS OF VARIANCE OF RESISTANCE PER UNIT AREA

1. Anodic sites

Triethanolamine

<u>Source of Variation</u>	<u>Degrees of Freedom</u>	<u>Sum of Squares</u>	<u>Mean Square</u>
Total	15	8,108,440	--
Runs	3	254,604	84,867
Treatment	3	7,069,347	2,356,425
Error	9	784,489	87,164

Standard Error of Mean = 147

2. Cathodic sites

Total	15	2,088,957	--
Runs	3	582,033	194,009
Treatment	3	1,130,426	376,805
Error	9	376,498	41,832

Standard Error of Mean = 102

Least Significant Difference = 390 ($t_{0.05-138}$)

TABLE XXVII

WEIGHT LOSSES OF ARMCO IRON STRIPS IN STATIC TESTS

Inhibitor	N (%)	Weight Loss* (mgms/dm ²)		
		<u>2 days</u>	<u>4 days</u>	<u>8 days</u>
Control	0.00	130.49	206.46	288.11
Aniline	0.01	146.24	209.82	302.58
	0.05	113.18	209.82	281.65
CHXA	0.01	109.30	187.60	276.23
	0.05	66.92	96.38	222.22
DIMAE	0.01	88.37	157.36	273.64
	0.95	37.47	84.24	170.54
ETHYLAMINE	0.01	80.88	159.17	269.77
	0.05	40.05	85.53	160.46
Morpholine	0.01	77.00	167.70	257.11
	0.05	41.09	79.33	154.00
Quinoline	0.01	109.82	163.82	247.54
	0.05	70.80	86.05	102.84
TEA ⁺	0.01	89.41	162.01	268.73
	0.05	25.84	30.23	121.96

* Average of weight losses for 4 strips

+ TEA was checked at 6 and 10 days.

Weight loss (6 days) = 36.43 mgms/dm²

(10 days) = 142.89 mgms/dm²

VITA

Allan Phillip David

Candidate for the Degree of

Doctor of Philosophy

Thesis: THE MECHANISM OF CORROSION INHIBITION BY ORGANIC AMINES
AS INTERPRETED BY OHMIC RESISTANCE FILM

Major Field: Chemical Engineering

Biographical:

Personal data: Born at Timmins, Ontario, May 15, 1924, the
son of Michael E. and Mary L. David.

Education: Attended grade school in Cochrane, Ontario;
graduated from Cochrane High School in 1941; received
Bachelor of Applied Science degree in 1950 and Master
of Applied Science degree in 1951 from the University
of Toronto, with a major in Chemical Engineering; com-
pleted requirements for Doctor of Philosophy degree in
May, 1959.

Professional experience: Employed by Diversey Corporation,
Chicago, 1951-1952; E. I. Dupont de Nemours, Chattanooga,
Tennessee, 1952-1954; Atomic Energy of Canada Ltd.,
Ottawa, Ontario, 1954-1956.

Member of: American Chemical Society; Phi Lambda Upsilon,
Sigma Xi.